Evaluation of Small-scaled Compressed Air Energy Storage

CARLOS OMAR RASGADO-MORENO

Evaluation of Small-scaled Compressed Air Energy Storage

Carlos Omar Rasgado Moreno

A Thesis presented for the degree of
Master of Science

Department of Engineering
University of Durham
United Kingdom

16 January 2020

Declaration

The work in this thesis is based on research carried out in Durham University. No part of this report has been submitted elsewhere for any other degree or qualification and it is all my own work unless referenced to the contrary in the text.

Acknowledgements

My gratitude to the Consejo Nacional de Ciencia y Tecnologia (CONACyT) and to the Secretaria de Energia (SENER) for this opportunity that let me grow in every aspect of my life. Also, I would like to thank to my family and Mr. Capuleto for their support.

CVU: 857038
Scholar: 639080
Scholarship: 495376

Abstract

The ongoing integration of renewable resources in the energy supply system has brought the problem of matching an intermittent supply to demand. This can be solved by energy storage and although there are currently solutions for this purpose, they tend to be either expensive or difficult to recycle. An alternative to these is to compress air using a compressor system, store the air, and then expand it through a turbine to produce energy when it is needed. This approach is called compressed air energy storage (CAES). Compressed air energy storage has been deployed in two large multi-megawatts plants in the world, in Germany (Huntorf 270 MW) and one in the USA (McIntosh 110 MW). However such a plant requires a large geological feature such as a salt cavern and considerable capital investment. To date there has been little interest in adapting compressed air energy storage plant to a small scale. This study explores the potential of such a system using cycle modelling to determine the potential outputs for such a system. The size, weight and cost of such a system is also evaluated. This thesis shows that at present small scale CAES is not competitive with other types of storage as the cost of the components is prohibitive.

Contents

List of Tables

List of Figures

Nomenclature

T	Temperature (^{o}C)
P	Pressure (bar)
$\dot{m}$	Mass flow (kg/s)
t	Time (s)
η	Efficiency
h	Heat transfer coefficient (W/(m^2 ^{o}C))
I_w	Insulation width (cm)
V	Volume (m^3)
γ	Isentropic exponent
R	Specific gas constant
ν	Specific volume (m^3/kg)
$\dot{Q}$	Heat flow
c	Heat capacity (kJ/(kg^{o}C))
ρ	Density (kg/m^3)
A	Area (m^2)
U	Overall heat transfer coefficient (W/(m ^{o}C))
k	Conductive heat transfer coefficient (W/(m ^{o}C))
H	Packed bed's height (m)
W	Work (J)
C	Energy cost (X currency/Wh)
D	TES diamater (m)
d	Rock diameter (m)
ε	Rock porosity

Subscripts:

ch	charging
dis	discharging
st	storage
in	inlet
out	outlet
t	expander
a	ambient
mc	mechanical
is	isentropic
$\dot{Q}$	Heat flow
g	gas
s	solid
ge	generator
i	initial
a	ambient
c	compressor
rt	round trip
f	fuel
ng	natural gas

Abbreviations:

UK	United Kingdom
s-c	Small-Scaled
ES	Energy Storage
RE	Renewable Energy
VRE	Variable Renewable Energy
CPS	Concentrated Solar Power
SMES	Super Magnetic Energy Storage
TES	Thermal Energy Storage
CAES	Compressed Air Energy Storage
A-CAES	Adiabatic Compressed Air Energy Storage
D-CAES	Diabatic Compressed Air Energy Storage
I-CAES	Isothermal Compressed Air Energy Storage
PV	Present Worth Value
EROEI	Existing Returned on Energy Invested

Chapter 1

Introduction

1.1 Renewable energy issues

In the 20th century the main energy sources were fossil fuels [12]. However, the excessive use of fossil fuels contributes to global warming and climate change [13]. Furthermore, with exponential population growth increasing the demand for energy and increasing concern regarding global warming [14] there is a push to increase the integration of renewable energy systems [15].

Renewable energy targets in the United Kingdom includes a reduction of 80% of carbon emissions by 2050 [16]. Also, The UK's Draft Integrated National Energy and Climate Plan [17] points out a reduction of 40% of carbon emissions for the period 2021-2030 compared to 1990 levels.

The *"Towards a New Energy Strategy"* [18] document explains the agreed actions in the European Union towards a sustainable future by 2020. It is important to point out that one of them, is the rise of renewable energy (RE) sources in the power supply, leaving aside the economic and environmental issues explained by Pimentel et al.[19], Mills et al. [20] point out the challenges related to the nature of variable renewable energy (VRE) and Sen and Ganguly [21] point out the role of skilled human resources in VRE generation.

1. Challenges related to the nature of VRE.

   (a) They are location-constrained.

   (b) VRE generator output. They are weather-driven.

   (c) They are unpredictable. There is an uncertainty in forecasts of future output.

   The points mentioned above can be illustrated briefly by solar energy production, first, the energy output would be bigger in countries near to

the Equator than in northern countries, challenge (a). Second, even in countries with high sun radiation, the energy production will decrease significantly during cloudy days and it will reach the highest production in sunny days, challenges (b) and (c).

2. Requirement of skilled human resources. Unlike fossil fuels-plants, RE systems required specific trained-workers in each RE sources. In other words, the operation and maintenance of wind turbines, would be different from solar panels [22].

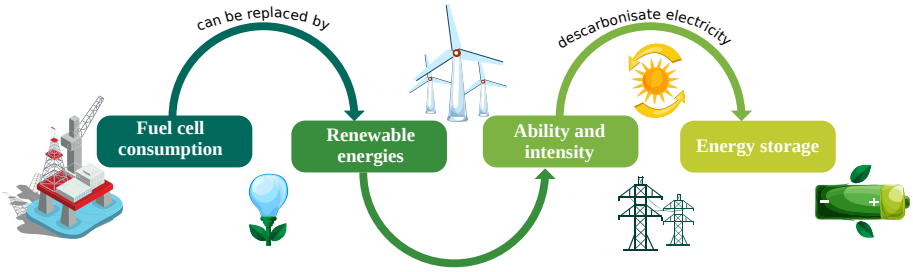

Figure 1.1: The role of energy storage. Icons designed by Freepik

1.2 The need for energy storage

In the past, the main objective of energy storage was to supply energy in peak hours [23]. Nowadays, the ongoing integration of renewable energy sources demand a mediator for the intermittent energy production and consumption [24]. Fig. 1.1 represents the role of energy storage and its background.

At industrial level, Budt et al. [9] state the need of energy storage to reduce the gap between production and consumption in monthly and seasonal cycles, which would provide flexibility in the energy production and transmission. In addition Belderbos et al.[24] argue the importance of reducing or replacing fuel-burning peaking plants by using a more 'environmental friendly' energy storage.

At consumer level, Siraganyan et al. [25] argues the feasibility of having an energy storage plant at home, where you can take energy from the grid during non-peak hours (in the night for example) and return it on peak hours. This idea, clearly contributes to the *"Towards a New Energy Strategy"* paper, where one of the main statements is to look for the integration of 'smart grids'. On the other hand, there is an overproduction during slow demand hours. Although the existing batteries are designed for this purpose, reducing their production cost and increasing their life cycle is an active area of research [26]. In the same way, an energy storage system at

home would reduce the dependence on large backup plants for the energy production [27].

Besides matching the supply and demand side, energy storage plays an important role in the following areas: electric supply and ancillary services [28].

1. Electric supply.

   Purchase inexpensive electric energy. During non-peak hours or periods when the price of electricity tends to be low, it would be feasible to charge the energy storage system in order to use it later or sell it when the price is high.

   Decentralize the energy generation. Energy storage contributes to the decentralization of electricity market by reducing the dependency in large central power station and approaching the power sources to the end user.

   Increase the generator's output. For an electric supply system, energy storage could be crucial to reduce the need to buy new central station generation capacity such as natural gas-fired cycle power plants.

2. Ancillary services.

   Reconcile momentary differences between supply and demand. The existing variations in the availability of variable renewable energies produce fluctuations in the energy supply. This fluctuations can occur in very short timescales such as minutes or seconds or large timescales such as hours or days. In addition the higher the share of electricity produced from VRE is, the larger become the fluctuations [29]. The integration of energy storage would reduce this fluctuations.

   Reserve capacity in the electric supply. The integration of VRE challenge the electric grid's ability to maintain reliable and economical system operations [30]. In this context energy storage could be available to operate if it is needed.

Furthermore, if renewable energy production is to be increased, apart from the decarbonization of electricity [31] it will be possible to replace the existing heating system run by oil or gas, with electrical heating.

Thus, the integration of RE will require an increase in reliability and reduction in the cost of energy at peak hours [23]. Therefore energy storage could be crucial to improve the development of renewable energies supplies [23, 27, 32].

1.3 Energy storage systems

As noted above, energy storage works as a mediator by unifying the generation and consumption process and as an optimizer in the electric supply and ancillary services. Besides Ter-Gazarian [31] points out that energy storage can play other functions due to its different characteristics of the supplied systems and it might depend on the storage system for example:

. Utility load levelling: make better use of existing plants and fuels.
. Storage for combined heat and power systems.
. Storage for electric vehicles.
. Reduce pollution in populated urban areas.

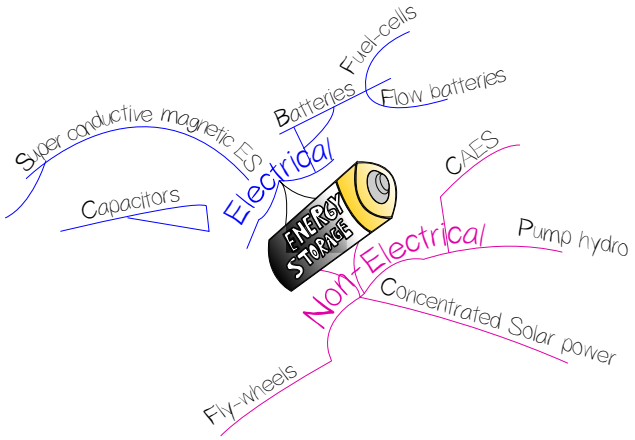

Figure 1.2: Most common electrical energy storage systems according to [1]

Elliman et al. [1] classify energy storage systems by the way the system converts the energy, either *electrical* and *non-electrical*. Fig. 1.2 shows the classification for the most common energy storage systems. Examples of electrical energy storage systems are batteries, capacitors and magnetic energy storage.

Batteries store energy in the form of chemical energy when a voltage is applied to them [33].

Capacitors store energy in the form of electrostatic charge, and can store it long periods of time without energy losses [34].

Superconductive magnetic energy storage (SMES), in this system the energy is kept in the form of a magnetic field, they are commonly used for a short term application [35].

In contrast, non-electrical energy storage systems convert other forms of energy (kinetic or thermal energy), such as pump-hydro storage, fly wheels, concentrated solar power and compressed air energy storage.

In *pump-hydro* storage, water from a lower level A is pumped to an upper level B into a reservoir. When the energy is needed, the water in the reservoir flows down and passes through a turbine to generate electricity [36].

Concentrated solar power (CSP) systems concentrate with mirrors or lens the heat from the sun into one specific focal point known as a power tower. Then, the stored heat enables the system to generate electricity when it is needed [37].

Flywheels basically keep kinetic energy through a rotational shaft connected to a motor/generator. There is an electrical input connected to the motor which makes spin the rotational shaft. By increasing the rotational speed with the motor/generator, the energy is stored in the form of kinetic energy. Then, the stored energy is converted to electricity again by slowing the flywheel's rotational speed with the motor/generator [1].

Compressed air energy storage (CAES) systems compress air from ambient conditions to pressure P. Then the air is kept in an air storage device, commonly a cavern or a vessel. This first step, can be recognized as the charging mode. Afterwards, when the energy is needed, the air from the storage device passes through an expander. The expander is coupled to a generator which produces electricity (the discharging mode). Fig. 1.3 summarizes the basic operation of a CAES system.

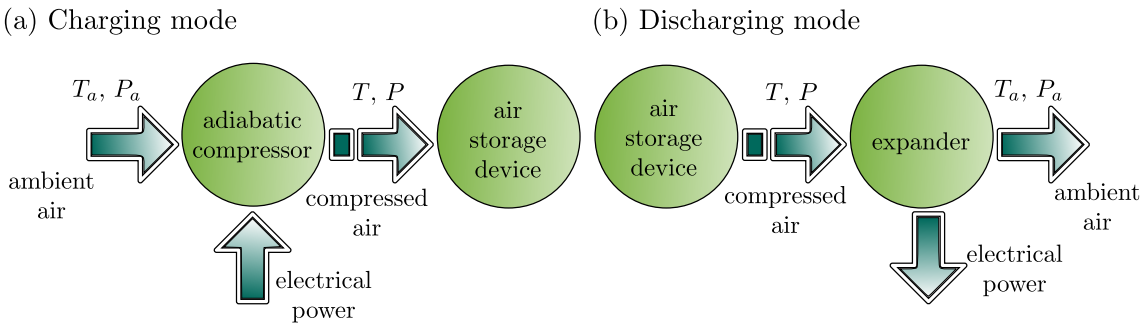

Figure 1.3: Basic CAES operation according to [7].

In addition, *thermal energy storage* (TES) systems store thermal energy by heating or cooling a storage medium. TES systems can be used for heating or cooling applications and power generation in combination with other storage systems such

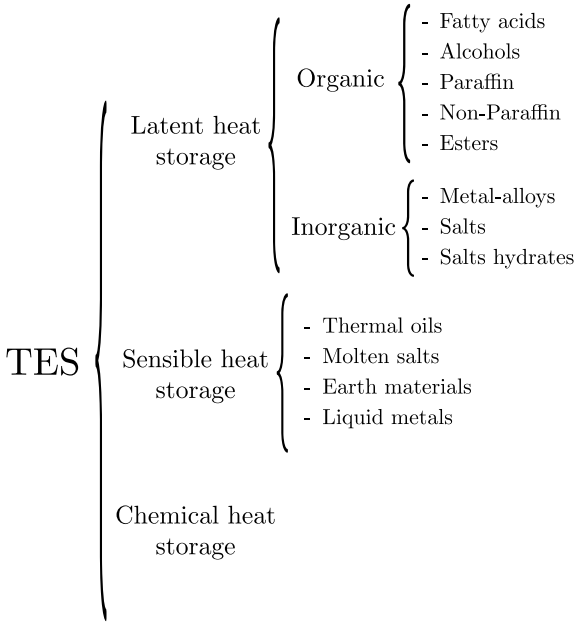

Figure 1.4: Heat storage material type based TES systems. [8].

as CAES or CSP. TES systems will vary depending on the heat source. Most commonly TES systems rely on solar thermal energy, geothermal energy, fossil-fuel power plants, nuclear power plants and industrial waste heat [8].

Thermal energy storage can be broadly classified according to the type of TES material selected for heat or cold storage [2]. It can be a sensible heat storage system, a latent heat storage system or a chemical heat storage system, Fig. 1.4 shows this classification. In sensible heat storage systems, the storage material stores heat energy in their heat capacity C_p. Examples of commonly used sensible heat storage materials are water, thermal oils, molten salts, earth materials and liquid metals.

In latent heat storage systems, the storage material stores heat energy in their latent heat capacity L during an isothermal process like phase change. Organic storage materials for latent heat storage commonly have their solid-liquid phase between 18 ^{o}C and 30 ^{o}C, examples of organic materials are paraffin, esters, alcohols and fatty acids. On the other hand, inorganic materials, such as metal-alloys and salts, operate in high temperatures where organic materials would have thermally disintegrated.

Chemical heat storage systems absorb and release heat through reversible reactions. The temperate range is between 200 ^{o}C and 400 ^{o}C. Their main characteristics are their highest thermal energy storage density and their long storage times. However chemical heat storage systems are still under development.

For reference, Table 1.1 shows the typical parameters of each energy storage system mentioned above.

System Type	Power	MWh	Discharge duration	Efficiency	Life time (years)
Batteries	< 200MW	< 200	Hours	75-90%	2-10
Capacitors	< 250KW	< 3	Sec/min	90-98%	30-40
SMES	0.3-3MW	< 3	Sec/min	90%	40
Pump-hydro	< 2GW	24GWh	Days	87%	40
CSP	0.1-200MW	< 2 GWh	Hours	80%	-
Flywheels	< 100KW	< 100	Sec/min	90%	20-30
CAES	< 300 MW	< 7GWh	Days	80%	30
Sensible heat storage	0.001-10 MW	< 50 kWh	Hours/days	50-90%	30-40
Latent heat storage	0.001-1 MW	< 150 kWh	Hours/days	75-90%	30-40
Chemical heat storage	0.01-1 MW	< 250 kWh	Hours/days	75-100%	-

Table 1.1: Typical parameters of energy storage systems [1] and TES systems [2].

1.4 Compressed air energy storage

Ideally, a compressed air energy storage system would take the overproduced energy from a renewable source to drive a compressor, then the compressed air will be stored in a vessel (potential energy). Later, in peak hours, the stored air can run a turbine in order to generate electricity. Furthermore, the heat produced by the compression can supply a cooling or heating system.

It is necessary here to clarify in more detail the operating system of a conventional compressed air energy storage plant. To do so, in their detailed review of compressed air energy storage, Budt et al. [9] considered that CAES systems might be divided into three main categories, depending on how the heat is added to the system, diabatic D-CAES, which use combustion before the expansion; Adiabatic A-CAES, which use a thermal storage to reuse the heat after compression and Isothermal I-CAES, which attempted to maintain the same air temperature during

the compression and expansion.

First, Kreid [38] and Haywood [39] describe a simple non-adiabatic or D-CAES as a modification of a Brayton cycle by adding an air storage to the system after the compression. Hence, heat is added to the air by burning fuel in the combustion chamber to run the turbine. Figure 1.5 (a) shows an overview of this modification. In addition, the main differences between each system for the purpose of this research are listed below:

- The turbine does not supply energy to the compressor like in a Bryton cycle.
- The main purpose of the combustion chamber is to add heat to the air before it enters in the turbine, in order to avoid frozen temperatures in the turbine and to improve the system efficiency.
- A compressed air energy storage plant may be divided into two main sub-processes, charging (air compression and storage) and discharging (energy production) mode. Whereas a Brayton cycle the air compression and expansion go simultaneously.

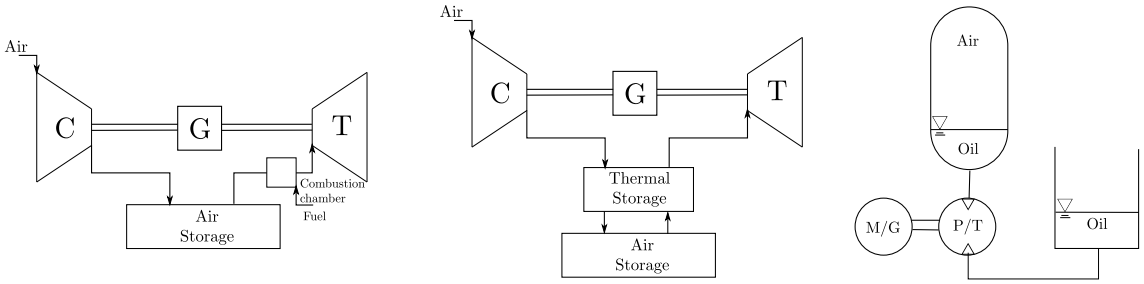

Figure 1.5: Different compressed air energy storage plants according to [9]. (C) compressor, (M/G) motor/generator, (T) turbine, (P/T) pump turbine.

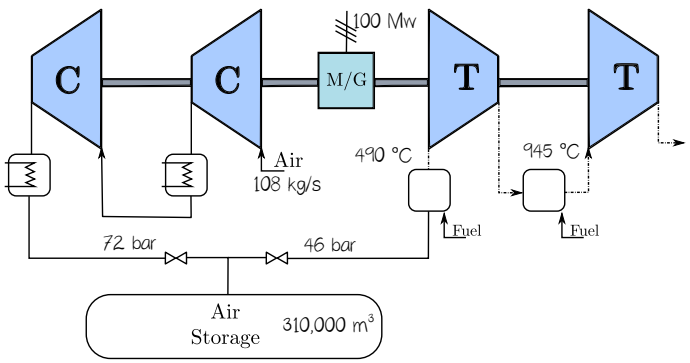

Figure 1.6: Huntorf plant diagram.

Moreover, the first CAES plant was built in the late 70s, the **Huntorf** plant, represented in Fig. 1.6, works by this system to supply peak hours in the north of Germany. According to Wolf [40] in the charging mode the Huntorf plant (290 MW) compressed air at 72 bar with a two-stage compression process with intercooling. Then, the air is kept in a 310,000 m^3 salt cavern. In the discharging mode, the air is throttled at 42 bar after leaving the cavern and heated up to 492 ^oC in a combustion chamber before enter into the high pressure turbine. Finally, the air is heated up again to 945 ^oC before entering in the low pressure turbine.

Unlikely the Huntorf plant, McIntosh plant (100 MW), the second plant built in the early 90s in the USA, works with a four-stage compression with intercooling to compress air at 72 bar in the charging mode [41] . Then, the air is kept in a 538,000 m^3 salt cavern. After, when the energy is needed, in the discharging mode, the air leaves the salt cavern and is throttled at 42 bar (similar to the Huntorf plant). Next, the air is preheated to 295 ^oC with a recuperator which carry the exhaust gases of the low pressure expander.

Ref	**System type**	**Temperature**	**Operating pressures**	**Efficiency**
Huntorf plant, [42]	D-CAES	Max. inlet temperature for LP is 945 ^oC, for HP is 550 ^oC	Max. pressure is 7.2 MPa, Operation pressure 4.2-6.6 MPa	Round trip efficiency 42%
Wolf and Budt, 2014 [7]	A-CAES	Operating temperature is 90-200 ^oC	Two configurations considered: one is 7.2 MPa and the other is 15 MPa	Round trip efficiency 56%
Quin and Loth, 2014 [43]	I-CAES	Ideal isothermal constant temperature	Max. pressure 1 MPa	More than 90 %

Table 1.2: Operation parameters and efficiencies for different CAES systems from [3].

Second, in A-CAES (see Figure 1.5 (b)), the combustion chamber is replaced by a thermal (TES) storage or a series of heat exchangers in order to heat up the air before the expansion. This model attempts to be feasible in terms of sustainability without a combustion chamber. Although several authors have proposed A-CAES designs for large and medium scale e.g. [44, 45, 40], thermal storage technology and high temperature compressors must be developed, because one of the main limitations of this model is the inability to achieve the same temperature rise as that with a combustion chamber. However, [7] developed a low-temperature A-CAES with a round trip efficiency of 56%. Table. 1.2 shows different operation parameters and efficiencies for D-CAES, A-CAES and I-CAES systems.

Third, a little variety of definitions of isothermal compressed air storage (see

Figure 1.5 (c)) have been suggested, Bud et al. [9] describes that I-CAES attempt to achieve isothermal compression and expansion by controlling the temperature of the air during each process. This attempt implies a slow compression and in all I-CAES known so far work with piston machinery. Some approaches have been developed such as the Sustain X project (2010) [46] or the analysis made by Qin and Loth [43], reaching a efficiency of 90% with the integration of wind energy.

1.5 Small-scale compressed air energy storage

As is described earlier, the decentralization of electrical energy will reduce the dependence on multi-megawatts plants and the energy losses and transmission's cost would decrease to the minimum.

Moreover, according to Pimentel et al.[22] one of the current challenges in the transition from fossil fuels to renewable energies in the U.S.A is the land resources required by renewable energies. For example, wind power requires 13,700 hectares to produced 1 billion kilowatt-hours of electricity per year but nuclear power requires 31 hectares to produce the same energy output [12].

Other challenges attached to large-scale renewable energy integration are: *technological challenges*, e.g. commonly in underdeveloped countries there is a la lack of infrastructure and trained personnel necessary to support the renewable energy power generation [47]; *economic challenges*, e.g. renewable energy technologies have high investment costs [48]; *social barriers*, there is evidence of local opposition against large-scale renewable energy generation, such as wind farms due to there are few economic benefits to local people [49]; *environmental impacts*, large-scale energy integration tend to have a negative impact in local ecosystems [50]; *regulatory barriers*, there is an existing need of energy policies concerning a sustainable development of renewable energies landscape management [48].

Therefore, small-scaled (s-c) energy storage can play an important role in the integration of renewable resources in the energy supply and current energy plants.

Although there are plenty of studies, models and proposals on compressed air energy storage e.g., [44, 45], they are mainly focused on medium/large-scaled plants. However, there are reports in some experimental procedures with s-c CAES. For example, Khamis et al. [51] reports empirical data from a simple A-CAES built with existing components (compressor, vessel and generator). In their experiment, they found that the system was able to produce 5.3 Volts with a compression ratio of 8 in 35 seconds. But, they did not go forward doing an exergy analysis of the system or sizing the system for a particular purpose. Furthermore, Venkataramani et al. [4] carried out an experimental investigation on small capacity adiabatic CAES system

by constructing a 400 L vessel surrounded by 27 L which served as insulation. In their experiment, they report a quasi-isothermal charging and storage. During the charging time, the water extracts the air's heat from the compression and it is kept at the same temperature during storage.

Also, the following points summarize the importance of small scaled energy storage:

Low risk. A small-scaled plant implies a low energy density. Therefore, it will be safer for future laboratory studies and operation.

Build experience. Nowadays, there are two multi megawatts plants, (Huntorf, Germany and McIntosh, USA), but it will be difficult to study them under different working conditions due to their big size. However, a small-scaled plant will provide more flexibility for further studies.

Microgeneration. Social housing providers are increasingly turning to microgeneration technologies to help reduce fuel costs and to meet any shortfall between renewable supplies and demand.

1.6 Research objectives

General objective. To evaluate the potential of small-scaled Compressed Air Energy Storage using cycle modelling to estimate efficiencies and a cost model using off-the-shelf components to evaluate how the proposed systems compares to battery technology.

Specific objectives.

- To identify the role of energy storage in the integration of renewable energy sources.
- To build a thermodynamic and economic model of a s-c CAES system.
- Tu build a numerical approach and run simulations to size the system.
- To evaluate different s-c CAES systems with off-the-shelf components.
- To compare a s-c CAES system with battery storage.

1.7 Summary

The ongoing integration of renewable resources in the energy supply system has brought the problem of matching an intermittent supply to demand. This can be solved by energy storage and although there are currently solutions for this purpose, they tend to be either expensive or difficult to recycle. An alternative to these is to

compress air using a compressor system, store the air, and then expand it through a turbine to provide energy when it is needed. This approach is called compressed air energy storage (CAES). Compressed air energy storage has been deployed in two large multi-megawatts plants in the world, in Germany (Huntorf 270 MW) and one in the USA (McIntosh 110 MW). However such a plant requires a large geological feature and considerable capital investment. To date there has been little interest in adapting compressed air energy storage plant to a small scale. This study explores the potential of such a system using cycle modelling to determine the potential outputs for such a system. The size, weight and cost of such as system is also evaluated.

Chapter 2

Thermodynamic model

2.1 Compression

As it was explained before in Chapter 1, it is convenient to analyse the CAES model in two process, the charging and discharging process. The charging process describes the work done by the compressor. This is the work input which drives the CAES system.

According to [52] the work done by the compressor can be expressed as a function of the air's mass m, the specific volume ν, the pressure ratio (P_2/P_1) and the specific heat ratio γ

$$W_c = m\nu_1 P_1 \frac{\gamma}{\gamma - 1}\left[\left(\frac{P_2}{P_1}\right)^{\frac{\gamma-1}{\gamma}} - 1\right] \tag{2.1}$$

Some authors, e.g. [45], [40], and [53], use Eq. 2.1 to describe the *charging mode*. P_2 and T_2 in Fig. 2.1 are the air's pressure and temperature delivered to the storage facility.

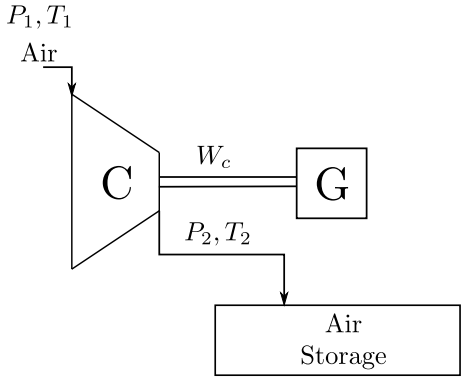

Figure 2.1: Sketch of the charging process.

2.2 Air Storage

The air's temperature and pressure will determine the charging time, energy losses during the storage and the initial conditions for the energy output during the discharging mode. Therefore, it is important to model the air dynamics inside the vessel during the compression, storage and expansion.

Temperature variation

According to [10] and [54] the mass and energy conservation of air flow inside the vessel are (the control volume in Fig. 2.2):

$$\frac{dm}{dt} = \dot{m}_{in} - \dot{m}_{out} \tag{2.2}$$

$$\frac{d}{dt}(mu) = \dot{Q} - \dot{W} + \Sigma \dot{m} h \tag{2.3}$$

where, u is the thermal energy, $\dot{Q}$ is the heat flux, $\dot{W}$ is the work done by the control volume, $\dot{m}$ is the mass flow. If $u = h - P\nu$, the left side of Eq. (2.3) can be written as

$$\frac{d}{dt}[m(h - P\nu)] = \frac{d}{dt}(mh) - \frac{d}{dt}(m\nu P) \tag{2.4}$$

$$= \frac{d}{dt}mh - P\frac{dV}{dt} - V\frac{dP}{dt} \tag{2.5}$$

substituting in Eq. (2.3) and taking in to account that there isn't any work done by the storage device,

$$\frac{d}{dt}mh = \dot{Q} + \dot{m}_{in}h_{in} + P\frac{dV}{dt} + V\frac{dP}{dt}$$

and assuming $h = c_p \Delta T$ where c_p is the specific heat,

$$\frac{dT}{dt} = \left[\frac{1}{mc_p}\right]\left[\dot{Q} + \dot{m}_{in}c_p(T_{in} - T) + P\frac{dV}{dt} + V\frac{dP}{dt}\right] \tag{2.6}$$

[10] use Eq. (2.6) to describe the energy conservation inside a cavern. However, the same model can be applied to a vessel as an air storage device.

Pressure variation

The pressure variation inside the vessel can be stated by the gas law [10]:

$$PV = zmRT \tag{2.7}$$

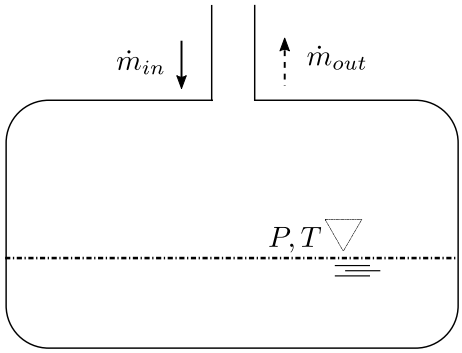

Figure 2.2: Sketch of the vessel pressure and temperature variation [10].

Where the pressure P times volume V equals, the mass m times temperature T and the gas constant R. For simplicity, the air can be consider an ideal gas with a compressibility factor $z = 1$. Differentiating Eq. 2.7,

$$\frac{dP}{dt} = \frac{1}{V}\left[RT\frac{dm}{dt} + Rm\frac{dT}{dt}\right] \tag{2.8}$$

considering the relations $R = c_p - c_v$, $dQ = c_p dT$ and $\gamma = c_p/c_v$,

$$\frac{dP}{dt} = \frac{1}{V}\left[\gamma RT_{in}m_{in} - \gamma RTm_{out} + (\gamma - 1)\dot{Q}\right] \tag{2.9}$$

Vessel's heat transfer

One of the main differences between small-scaled and large-scaled compressed air energy storage plants is the storage mechanisms. For the small-scaled CAES it might be convenient to store the air in a vessel rather than a cavern. He et al. [10] propose a heat transfer model for the energy losses in the cavern considering the type of cavern's rock. However, the lumped-heat capacity analysis can be used to model the air's temperature lost during the storage time.

Considering a constant temperature around a body, and assuming that the internal resistance of the body is negligible in comparison with the external resistance. According to Holman [55] the heat loss of the vessel is evidenced as a decrease in the internal energy of the body with temperature T with respect to the ambient temperature T_a an the overall heat transfer coefficient U:

$$q = \overbrace{UA(T - T_a)}^{\text{heat loss from the body}} = \underbrace{-c\rho V\frac{dT}{dt}}_{\text{Internal energy of the body}} \tag{2.10}$$

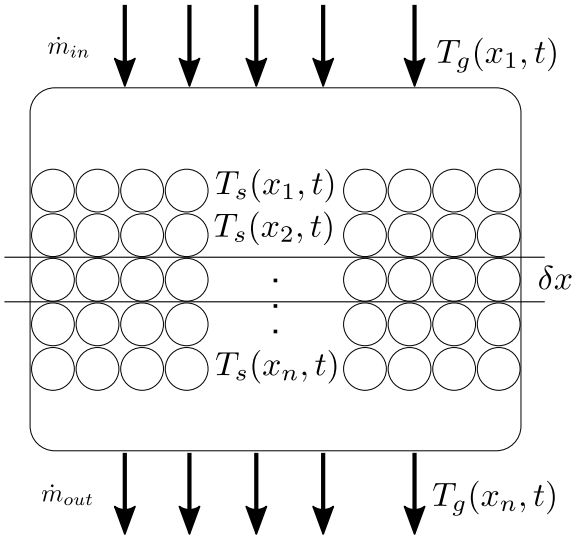

Figure 2.3: Sketch of a packed bed thermal storage system according to [6].

Solving the equation,

$$T = \left(e^{\frac{-UA}{c_p V}t}\right)\left(T_0 - T_a\right) + T_a \tag{2.11}$$

where T_0 is the initial body temperature.

2.3 Thermal storage

Often in energy storage systems, 20% to 40% of the stored energy is lost [28]. In order to reduce the the air's temperature loss during the storage time, a thermal storage unit could be considered. In compressed air energy storage systems, during the charging time, when the air's temperature increases by the effect of the compression, the thermal storage unit would extract heat from the air, this would reduced the energy loss with the surroundings and the extracted heat would be used later to rise the air's temperature during the discharging time.

The thermal storage in this work is considered to be a packed bed as it is shown in Fig. 2.3. Shumann et al. [56] describe the heat transfer process of a fluid at temperature T_g flowing through a porous prism T_s by the following system of partial differential equations:

$$\frac{\partial T_g}{\partial t} + \upsilon\frac{\partial T_g}{\partial x} = \frac{-UA}{(c\rho)_g\varepsilon}(T_g - T_s) \tag{2.12}$$

$$\frac{\partial T_s}{\partial t} = \frac{UA}{(c\rho)_s(1-\varepsilon)}(T_g - T_s) \tag{2.13}$$

where, Equations (2.12) and (2.13) describe the heat transfer processes of the heat

transfer fluid (air's temperature during charging or discharging) and the solid material (thermal storage unit) respectively. Also, U is the heat transfer coefficient between the heat transfer fluid and the solid particles; ε is the solid's porosity; c is the heat capacity; ρ is the density; A is the particle area per unit bed volume determined as

$$A = \frac{6(1-\varepsilon)}{d}$$

If the air is kept at the same temperature at the entry of the packed bed $T_g = T_{gi}$ for all time at $x = 0$. And the initial packed bed temperature at t=0 will be $T_s = T_{si}$. For simplicity, consider $\alpha_2 = \frac{-UA}{(c\rho)_g \varepsilon}$ and $\alpha_1 = \frac{UA}{(c\rho)_s(1-\varepsilon)}$
In order to complete the system, from Eq. (2.13), the solid's temperature at $x = 0$ will be

$$\begin{aligned} \frac{dT_s}{dt} &= -\alpha_1(T_s - T_g) \\ T_s &= T_{gi} + (T_{si} - T_{gi})e^{-\alpha_1 t} \end{aligned} \tag{2.14}$$

In the same way, for the fluid temperature at $x = vt$, $T_s = T_{si}$

$$\begin{aligned} \frac{dT_g}{dt} &= -\alpha_2(T_g - T_s) \\ T_g &= T_{si} + (T_{gi} - T_{si})e^{\alpha_2 t} \end{aligned} \tag{2.15}$$

2.4 Expansion

Unlike the *charging mode*, where the work is on the air, in the *discharging mode* the work is done by the air. Therefore, the equation of state for a perfect gas enable Eq. 2.1 to be written as

$$W_t = m\frac{\gamma}{\gamma - 1} R T_2 \left[1 - \left(\frac{P_2}{P_1}\right)^{\frac{\gamma-1}{\gamma}}\right] \tag{2.16}$$

Where, T_2 is the air's inlet temperature, P_2 the outlet pressure and P_1 the vessels minimum pressure.

The final electrical work supplied by the generator would be,

$$W_{ge} = W_t \eta_t \eta_{ge} \tag{2.17}$$

where, η_t is the expander's efficiency and η_{ge} is the generator's efficiency.

2.5 Efficiency

Traditionally, the efficiency η of a energy cycle is defined as the energy out E_{out} divided by the energy in E_{in},

$$\eta = \frac{E_{\text{out}}}{E_{\text{in}}} \tag{2.18}$$

In order to compare a CAES unit with other electrical storage options, (see Fig 1.2) Barnes and Levine [23] suggest a round trip electrical storage efficiency η_{rt} calculated as the electricity output divided by the electricity input:

$$\eta_{rt} = \frac{E_T}{E_c + \eta_{ng} E_f} \tag{2.19}$$

where E_T is the electricity delivered by the generator in the discharging mode, E_c the electricity needed to run the compressor in the charging mode, and $\eta_{ng} E_f$ the amount of electricity that could be made by heating up the air with natural gas.

2.6 Summary

This Chapter have exposed a basic approach to analyze a CAES system integrated by a compressor, expander, storage unit and thermal storage.

Based on the equations summary from Table 2.1, two thermodynamic models can be developed for the CAES systems evaluation, steady or unsteady. Table 2.2 presents the main advantages and disadvantages considered in this work for the two models. On the one hand, the steady approach give a general overview of the system when most of the operation data is available (e.g. operation times, mass flow, storage volume), so it can be computed the work done by the compression and the expander. On the other hand the unsteady approach allowed the complete design and operation analysis of the CAES systems from scratch. This model can approximate charging times, discharging times, energy loss with the surroundings and the system efficiency.

Compression	$W_c = P_1 V_1 \frac{k}{k-1}\left[\left(\frac{P_2}{P_1}\right)^{\frac{k-1}{k}} - 1\right]$	(2.1)
Air storage	$\frac{dm}{dt} = \dot{m}_{in} - \dot{m}_{out}$	(2.3)
	$\frac{dT}{dt} = \left[\frac{1}{mc_p}\right]\left[\dot{Q} + \dot{m}_{in}c_p(T_{in} - T) + P\frac{dV}{dt} + V\frac{dP}{dt}\right]$	(2.6)
	$\frac{dP}{dt} = \frac{1}{V}\left[\gamma R T_{in} m_{in} - \gamma R T m_{out} + (\gamma - 1)\dot{Q}\right]$	(2.9)
Thermal storage	$\frac{\partial T_g}{\partial t} + \upsilon\frac{\partial T_g}{\partial x} = \frac{-UA}{(c\rho)_g \varepsilon}(T_g - T_s)$	(2.12)
	$\frac{\partial T_s}{\partial t} = \frac{UA}{(c\rho)_s(1-\varepsilon)}(T_g - T_s)$	(2.13)
Expansion	$W_t = m\frac{k}{k-1}RT_3\left[1 - \left(\frac{P_1}{P_2}\right)^{\frac{k-1}{k}}\right]$	(2.16)

Table 2.1: Basic CAES mathematical model

	Advantages	**Disadvantages**
Steady model	- It is useful for drafting systems designs. - Does not require a lot computational power to be computed. - It gives a general overview of the system.	- Requires more data to run, e.g. operation times. - It does not compute energy loss with the surroundings. - It is not possible to analyse the thermodynamics inside the vessel.
Unsteady model	- It gives a better approach of the system's operation and performance. - When the computational model is developed, it is flexible and user friendly to run different simulations. - It gives a detailed overview of the system.	- Requires considerable computational power to run. - Depending in the desirable accuracy an system's variables the simulation time will vary, eg. 10 minutes, 2 hours, 12 hours, etc. - It requires a numerical computing environment to solve the unsteady equations.

Table 2.2: Advantages and disadvantages of the Steady and Unsteady models .

Chapter 3

Economic model

A thermodynamic model for a small-scaled compressed air energy storage (CAES) plant was developed in the previous chapter. In this chapter, it is introduced a model to asses the profit of CAES system according to [31]. This model considers a stakeholder who own the energy storage system. Therefore he will get the profit for charge the energy storage system when electricity prices are low and discharge in peak energy demand hours or when electricity prices are high.

3.1 Price of energy

Power is always the rate flow of energy (Watt=Joule $\times$ seconds). The fact that power is a *flow*, its total cost should be measured in money per hour [57]:

$$\text{(money per hour) per W} = \frac{(£/h)}{W} = \frac{£}{Wh}$$

where $£$ is the cost of energy. From, the equation above, the profit P of a CAES plant can be stated as follows

$$Profit = C_{\text{sell}} E_{\text{out}} - C_{\text{buy}} E_{\text{in}} \tag{3.1}$$

where $C_{\text{buy}}, C_{\text{sell}}$ are the cost of energy consumed and produced, respectively .

The ratio of pricing to round-trip efficiency

From the round trip efficiency equation. (2.18), $E_{\text{out}} = \eta E_{\text{in}}$, Eq. (3.1) can be written as follows,

$$Profit \;\; = \;\; E_{\text{in}} \left(\eta C_{\text{sell}} - C_{\text{buy}}\right) \tag{3.2}$$

considering a cost ratio stated by the cost of energy $r_c = C_{\text{sell}}/C_{\text{buy}}$ the profit equation (3.2) can be written in terms of the efficiency and energy costs,

$$Profit \;\; = \;\; E_{\text{in}} C_{\text{buy}} \left(\eta r_c - 1\right) \tag{3.3}$$

According to equation (3.3) it can be noticed that in order to make the system profitable the round trip efficiency times the cost ratio should be bigger than the unity, $\eta r_c > 1$.

3.1.1 Present worth value

In any investment it is important to consider the value of the money over the time in order to estimate the internal rate of return. To do so, the present worth value is a good approach [58],

$$PV(i) = \sum_{n=0}^{N} \frac{A_n}{(1+i)^n} \tag{3.4}$$

where

N = Time.

A_n = Cash flow.

i = discount rate.

3.2 Summary

To sum up, the present worth value (PV) is the current value of a future sum of money or stream of cash flows given a specified rate of return. Determining the PV for the CAES system will state the system profitability during its life cycle and it could be possible to compare the CAES plant with other energy storage facilities.

Chapter 4

Numerical approach

Two different approaches for the thermodynamic model explained in Chapter 2, one steady and one unsteady, were made for the proposed compressed air energy storage system with two different software respectively, explained below. During the design process, the starting point was the steady modelling. It was used to build simple CAES systems with hypothetical given conditions such as operation times, efficiencies, heat loss, etc. Then, the unsteady modelling was used analyse in more detail the CAES systems and to approximate the given conditions previously in the steady modelling.

4.1 Steady model

The *steady model* focuses on the power required and delivered by the system. It computes the power needed to run the compressor and the power output delivered by the expander. This analysis can be done with Cycle-Tempo 5. Cycle-Tempo is an object-oriented thermodynamic software which allows the user to analyze thermodynamic systems by building a block model and stating the system's parameters [59]. Cycle-Tempo builds a system of equations based in mass and energy balances, which is a matrix, then it solves it and display the results.

Fig. 4.2 shows a Cycle-Tempo model for a simple adiabatic compressed air energy storage system. Cycle-Tempo builds a system matrix based on the operation parameter for each component in the system, Fig. 4.1 shows a general approach for each component. Then, with the system matrix, the mass flows and power outputs are calculated simultaneously. The equations prepared are:

for the *charging* time:

1. Mass balance of the compressor.
2. Mass balance of the air source.

Compression	$W_c = P_1 V_1 \frac{k}{k-1}\left[\left(\frac{P_2}{P_1}\right)^{\frac{k-1}{k}} - 1\right]$	(2.1)
Expansion	$W_t = m\frac{k}{k-1} R T_3 \left[1 - \left(\frac{P_1}{P_2}\right)^{\frac{k-1}{k}}\right]$	(2.16)

Table 4.1: Steady model equations.

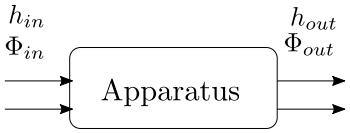

Figure 4.1: Energy and mass balance of an apparatus in Cycle-Tempo.

3. Energy balance of the compressor.
4. Energy balance of the air source.
5. Energy balance of the motor.

for the *discharging* time:

1. Mass balance of the turbine.
2. Mass balance of the stack.
3. Energy balance of the turbine.
4. Energy balance of the stack.
5. Energy balance of the generator.

4.2 Unsteady model

An unsteady model gives a general approach to analyse a CAES plant when it is known the operation time and the input and output variables for the charging and discharging mode. However, CycleTempo is unable to compute operation times, simulate the system in each time-step and it cannot capture events such as the change from charge to discharge.

Therefore, in order to compute an accurate energy balance, it is important to develop a dynamic model for a CAES plant. In Chapter 2 the equations and variables implied in the operation of a CAES plant were explained. In this Section, the time

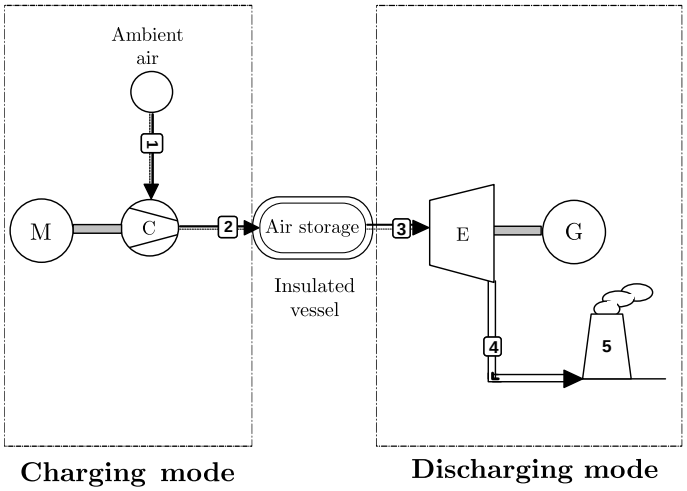

Figure 4.2: CycleTempo block model: A-CAES. (M) motor, (C) compressor, (E) expander, (G) generator.

dependent equations are linked through an object-oriented numerical tool called Simscape from Matlab 2018a.

Matlab (matrix laboratory) is a numerical computing environment and a programming language [60]. Simscape is a Matlab tool box which enables you to build physical models based on physical connections.

For the purpose of this research Simscape was selected for the reasons explained below:

1. Rigour. Simscape allows the user to build the model in the command window and just set up the initial conditions. The program itself solved the equations implied in the model. So, the user does not have to look upon numeric or algebraic solutions for the system of equations.

2. Flexibility. When working with differential equations, any new variable or condition added to the system will change the solution. Moreover, it can be time consuming to solve the system of equations which model a CAES plant. Also the rigour of the solution would decrease depending in the methodology used to solve the new system of equations. The current model explained below is based on basic operation components: compressor, vessel and expander. Further studies will require to include valves, pipes, heat exchangers, etc.

3. Non-linear behaviour. Simscape has the capacity to solve non-linear differential equations and turn on and off components.

Simscape was used to approximate the differential equations (2.6) and (2.9) for the air's temperature and pressure variations inside the vessel. It can be mentioned

Compression	$W_c = P_1 V_1 \frac{k}{k-1}\left[\left(\frac{P_2}{P_1}\right)^{\frac{k-1}{k}} - 1\right]$	(2.1)
Air storage	$\frac{dm}{dt} = \dot{m}_{in} - \dot{m}_{out}$	(2.3)
	$\frac{dT}{dt} = \left[\frac{1}{mc_p}\right]\left[\dot{Q} + \dot{m}_{in} c_p (T_{in} - T) + P\frac{dV}{dt} + V\frac{dP}{dt}\right]$	(2.6)
	$\frac{dP}{dt} = \frac{1}{V}\left[\gamma R T_{in} m_{in} - \gamma R T m_{out} + (\gamma - 1)\dot{Q}\right]$	(2.9)
Expansion	$W_t = m\frac{k}{k-1} R T_3 \left[1 - \left(\frac{P_1}{P_2}\right)^{\frac{k-1}{k}}\right]$	(2.16)

Table 4.2: Unsteady model equations.

that Eq. (2.6) and (2.9) are deduced from the mass and energy balances (2.2) and (2.7) proposed by [10].

In the same manner, each Simscape element has its own pre-programmed energy balance equations [60]. Therefore, from Fig. 4.4, Simscape will build a system of equations based on the mass and energy balances for each block, and it will approximate the temperatures and pressures in each step in time.The time step of the dynamic simulation is in seconds.

Furthermore, to cycle-model a CAES system, a Simscape model was built for each step in the cycle; charging, storage, discharging and the resting time where the system goes back to the initial conditions.

In addition, the operation parameters and the Simscape's models are integrated in a Matlab script. Fig. 4.3 illustrates the Matlab's script algorithm.

The *gas* and *thermal* systems were selected to model the CAES plant, due to the dynamic analysis relies on the air's pressure and temperature over time. A simple approach to a CAES system is showed on Fig. 4.4.

First, in the charging mode on Fig. 4.4 the *gas* system computes the isentropic compression by setting a constant mass flow $\dot{m}_{in}$ from ambient pressure P_a and temperature T_a to P_2 and T_2. See Fig. 4.5. Then, the air fills the vessel of volume V which is at a pressure P_v and temperature T_v until it reaches the pressure P_2 in a charging time t_{ch}.

The *thermal* system models the vessel's heat transfer with the environment,

considering I_w cm of insulation and a heat transfer coefficient h based on the free convection for a horizontal cylinder [55].

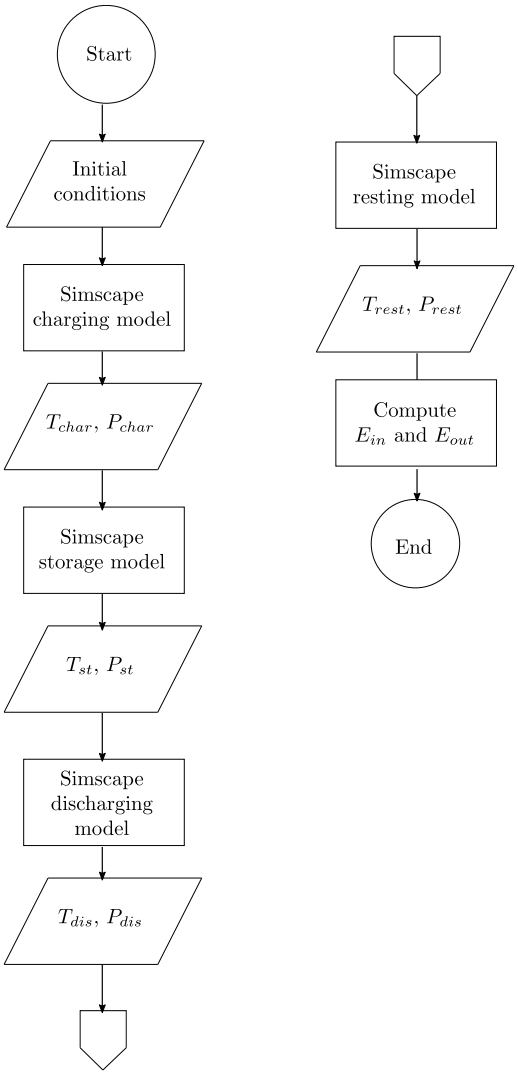

Figure 4.3: Matlab script flow diagram configuration.

Second, in the storage mode the *thermal* system models the heat $\dot{Q}$ lost during the storage time t_s. It can be noticed that in the storage mode the pressure P_v decreases until $T_v = T_a$ and the storage time t_s is stated by the user in the initial conditions.

Third, in the discharging mode, the air will be delivered to the turbine at a constant pressure and mass flow, therefore the same criteria from the charging mode is followed by setting a constant mass flow rate $\dot{m}_{out}$.

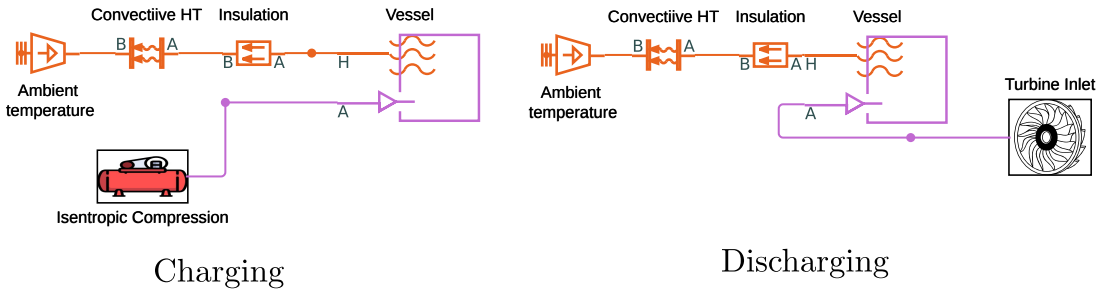

Figure 4.4: Simscape's configuration for the charging, storage and discharging mode

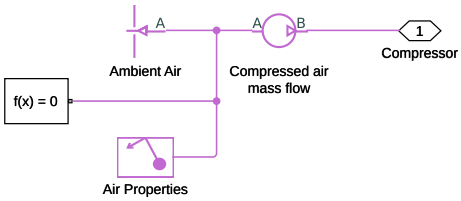

Figure 4.5: Simscape compressor's configuration

4.2.1 Unsteady model verification and validation

The experiments carried out by Venkataramani et al. [4] studied the performance of an adiabatic small-scaled compressed air energy storage plant which took the electrical energy for a wind power system to run a scroll compressor. The air, was then kept in a vessel surrounded by 27 litres of water and insulated with glass wool thickness of 20 mm. Fig. 4.6 shows the main system components for the CAES system.

Assuming an isentropic compression and expansion process, the experimental set up of Fig. 4.6 can be simulated with a Simscape model. Fig. 4.7 shows the structure of the Simscape model for the CAES system, the main components of the CAES system are: scroll compressor, insulated air's vessel by a mass of water and the scroll expander.

Experimental parameters for the simulation are listed on Table 4.3. Three different mass outlet flows m_{out} were simulated, 0.005 kg/s, 0.075 kg/s and 0.01 kg/s.

Fig. 4.8 shows the simulated air's temperature and pressure variations inside the vessel. During the charging time it can be noticed that the temperature varied from 20 ^{o}C to 22 ^{o}C. Simulations results match with the reported quasi-isothermal charging mode. In the storage mode the air temperature was set to be constant.

In order to evaluate the accuracy of the Simscape model, the infinity norm was used to compute the error. The infinity norm of a vector is defined as the largest

magnitude among each element of a vector $\vec{v}$:

$$||\vec{v}||_\infty = max\{|v_i| : i = 1, 2, ..., n\}$$

Computing the infinity norm, the error can be stated as follows,

$$error = \frac{||\vec{v}_{apx} - \vec{v}_{exp}||_\infty}{||\vec{v}_{exp}||_\infty}$$

where $\vec{v}_{apx}$ is the approximation vector and $\vec{v}_{exp}$ the vector of experimental values for pressure temperature and power output.

For the pressure and temperatures simulations in Fig. 4.9 and 4.10 the error was 0.39 %. It can be pointed out a change of η_t during the discharging mode which is difficult to approximate accurately with the data reported by [4].

The 0.39 % of error computed from the data presented below provides 2 significant digits of confidence to run simulations with different configuration systems.

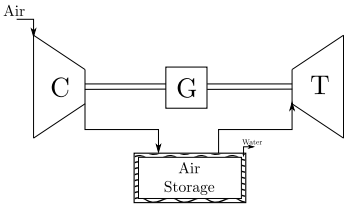

Figure 4.6: Experimental components for the CAES system carried by [4]. (C) compressor, (G) motor/generator, (T) expander.

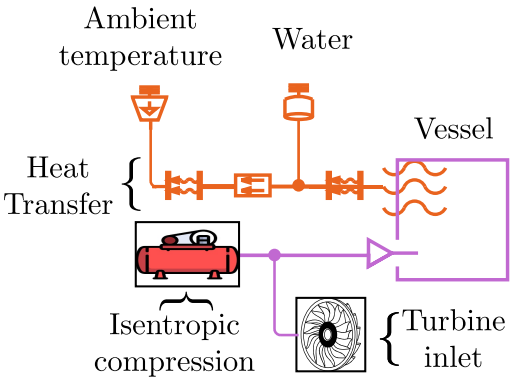

Figure 4.7: Simulation model for [4].

Parameter	value	Parameter	value	Parameter	value
Charging mode		*Storage*		*Discharging mode*	
Air mas flow rate (kg/s)	m_{in}	Air storage vessel volume (m^3)	4	Air mas flow rate (kg/s)	m_{out}
Ambient temperature (°C)	20	Water volume (m^3)	0.027	*Expander*	
Compressor		Max pressure in vessel (bar)	8	Inlet pressure (bar)	2
Compression pressure (bar)	8	Min pressure in vessel (bar)	2	Isentropic efficiency	0.85
Isentropic efficiency	0.85	Heat transfer coefficient ($W/(m^2\ K)$)	7.13	Mechanical efficiency	$\eta(t)$
Mechanical efficiency	0.85	Thermal conductivity ($W/(m^2\ K)$)	0.088		
		Insulation width (cm)	20		

Table 4.3: Simulation data set up according to [4].

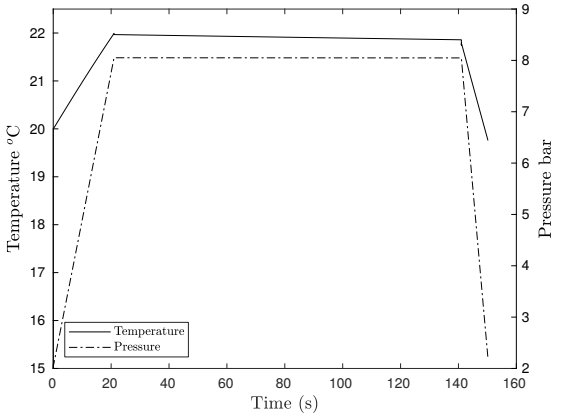

Figure 4.8: Simulated air's temperature and pressure inside the vessel for the experiment carried by [4].

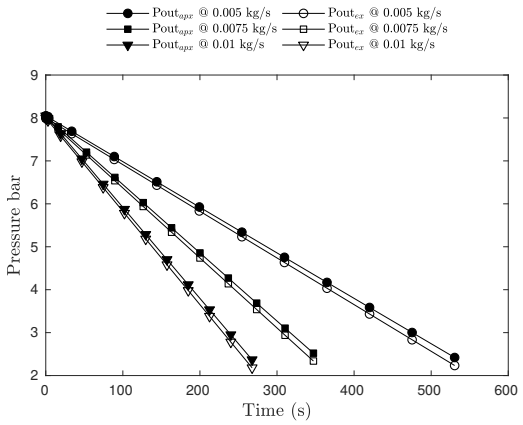

Figure 4.9: Simulated ($Pout_{apx}$) and experimental ($Pout_{exp}$) vessel's pressure durimg discharging mode.

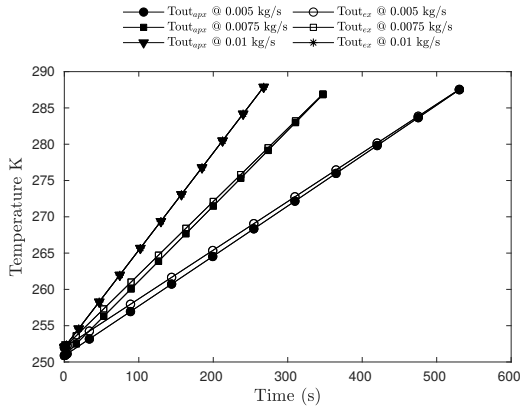

Figure 4.10: Simulatated ($Tout_{apx}$) and experimental ($Tout_{exp}$) air temperature inside the vessel during discharging.

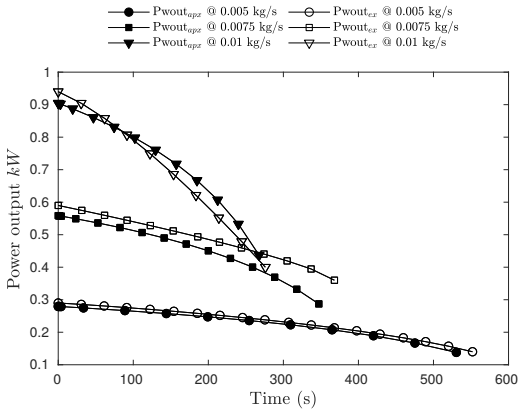

Figure 4.11: Experimental ($Pwout_{exp}$) and simulated ($Pwout_{apx}$) power output at different mass outlet

4.3 Summary

In this Section, two numerical approaches were computed for the steady and unsteady models, CycleTempo for the steady model and Simscape for the unsteady model. Cycle-Tempo allows the user tu build thermodynamic systems based on block models. Cycle-Tempo could be a good starting point for design and analysis of CAES systems. The main restrictions of Cycle-Tempo is that it is unable to compute operation times and heat loss with the surroundings. On the other hand, Simscape is a more sophisticated engineering software, it can compute non-linear equations and unsteady equations. Simscape can provide a better approach of the system's operation and performance.

Chapter 5

D-CAES and A-CAES

5.1 Components

In this section adiabatic and diabatic small-scaled compressed air energy storage models are presented. Based on a desktop web search, this study considered the sizes of off-the-self components on the market that can be used to build the system:

The *Atlas Copco LT compressor* was considered to this systems due to its solid reliability, low running costs and consistent air flow, different compressor's with general details are listed in Table 5.1.

Type	Maximum working pressure	Volume flow		Motor rated power	Sound pressure level		Container volume[3]	Approx. Weight	Dimensions L×W×H
	bar	l/s	m³/min	kW	db(A)		L	kg	mm
LE/LT - Piston compressors									
LE 2–10/90	10	3.40	0.20	1.5	80	65	90	85	1118×510×1017
LE 3–10/90	10	4.40	0.26	2.2	81	66	90	89	1118×510×1017
LE 5–10/250	10	8.40	0.50	4.0	81	66	250	150	1852×510×1082
LE 7–10/250	10	11.70	0.70	5.5	82	70	250	191	1852×592×1162
LE 10–10/250	10	15.70	0.94	7.5	83	70	250	203	1852×592×1162
LE 15–10/250	10	18.60	1.12	11.0	86	-	250	330	1852×790×1200
LE 20–10/250	10	23.90	1.43	15.0	86	-	250	360	1852×790×1200
LT 2–15/90	15	3.10	0.19	1.5	80	65	90	100	1118×533×1017
LT 3–15/90	15	4.00	0.24	2.2	81	66	90	104	1118×533×1017
LT 5–15/250	15	6.70	0.40	4.0	81	66	250	170	1852×533×1082
LT 7–15/250	15	9.20	0.55	5.5	82	70	250	211	1852×606×1162
LT 10–15/250	15	11.70	0.70	7.5	83	70	250	223	1852×606×1162
LT 2–20/90	20	2.10	0.13	1.5	80	65	90	100	1118×533×1017
LT 3–20/90	20	2.90	0.17	2.2	81	66	90	104	1118×533×1017
LT 5–20/250	20	5.00	0.30	4.0	81	66	250	170	1852×533×1082
LT 7–20/250	20	6.70	0.40	5.5	82	70	250	211	1852×606×1162
LT 10–20/250	20	9.10	0.55	7.5	83	70	250	223	1852×606×1162
LT 15–20/250	20	15.10	0.91	11.0	86	73	250	333	1852×830×1980
LT 20–20/250	20	18.00	1.08	15.0	86	73	250	361	1852×830×1980
LT 3–30	30	2.50	0.15	2.2	81	-	-	49	686×533×497
LT 5–30	30	4.40	0.26	4.0	81	-	-	51	686×533×497
LT 7–30	30	6.40	0.38	5.5	82	-	-	90	860×606×600
LT 10–30	30	8.50	0.51	7.5	83	-	-	102	932×606×600
LT 15–30	30	9.30	0.56	11.0	83	-	-	166	1024×682×675
LT 20–30	30	17.00	1.02	15.0	89	-	-	194	1103×713×675

Table 5.1: Atlas Copco compressors details [5].

The *Roy E. Hanson* ASME pressure vessels company was selected because it has many variations of custom standard air receivers and many air tanks in stock.

The *airsquared expander* was one of the few small expanders on the market which fits the characteristics of the plant design. The Airsquared company was selected because it is an industry leader in oil-free scroll design and manufacturing.

5.2 Initial parameters

The small-scaled Compressed Air Energy Storage system has been sized to fit into a garage in order to contribute to the energy supply of a small building, e.g. a house.

Fig. 5.1 presents the proposed small-scaled system's layout according to the potential components explained above. The system's parameters are listed on Table 5.2 which are based mainly on the electricity cost-cycle in Fig. 5.2 and the following considerations:

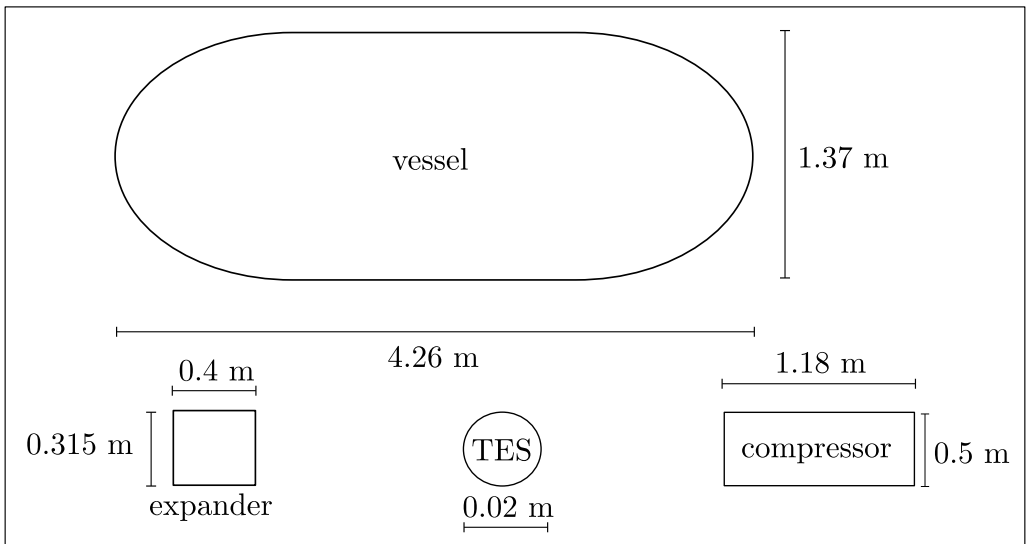

Component	**Company**	**Model**	**LxWxH (m)**	**Weight (kg)**	**Cost £**
Compressor	Atlas Copco	LT2-15	1.18 x 0.533 x 1.017	100	4,000
Vessel	Roy E. Hanson	# 165	4.26 x 1.37 x 1.57	1190.2	10,211
Expander	airsquared	E22H038A-SH	0.427 x 0.315 x 0.287	-	13, 427
TES	-	-	0.02 x 0.02 x 1.2	100	300

Figure 5.1: SC-CAES system's layout proposal.

△ The charging and discharging time. According to Wang et al. [61] the higher electricity prices during the day are on peak energy demand hours which tend

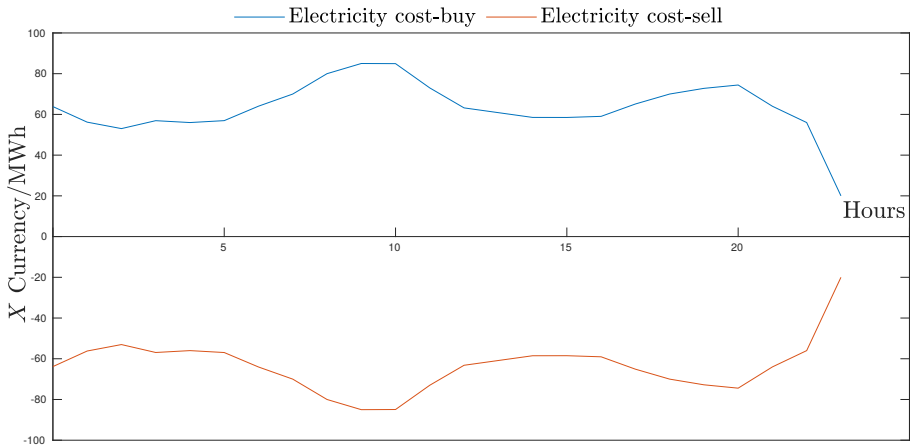

Figure 5.2: Electricity cost-cycle during 24 hours based on [11]

to last 1 to 2 hours. The proposed CAES system was designed to contribute to this energy demand for 40-60 minutes.

- △ The storage time was selected to be 6 hours. The CAES unit was considered to be charged in non-peak hours (mid-day) and store the energy until peak hours (evening) [61]. For this reference see the energy 24 hours cost-cycle in Fig. 5.2.
- △ The charging/discharging pressure and mass flows $\dot{m}$. The minimum operation pressure has been selected according to the technical data of the compressor mentioned above. Therefore, the vessel have been thought to be full by compressing air at 15 bar and throttled at 9 bar in the discharging mode.
- △ Due to the CAES system was designed to contribute to the energy supply of a small building unit, the vessel volume V was fixed to the potential available space founded in a basement, garage, backyard, etc. A 5 m^3 vessel was considered.
- △ The entry parameters of the combustion chamber (fuel mass flow, reaction pressure and reaction temperature) were based on the technical data available for the *airsquared* expander [62].

Parameter	value	Parameter	value	Parameter	value
Charging mode		*Storage*		*Discharging mode*	
Air mas flow rate (kg/s)	0.006	Air storage vessel volume (m^3)	5	Air mas flow rate (kg/s)	0.006
Ambient temperature (^{o}C)	15	Max pressure in vessel (bar)	15	*Expander*	
Compressor		Min pressure in vessel (bar)	9	Inlet pressure (bar)	9
Compression pressure (bar)	15	Heat transfer coefficient (W/(m^2 K))	7.13	Inlet temperature (^{o}C)	300
Isentropic efficiency	0.87	Thermal conductivity (W/(m K))	0.088	(D-CAES only)	
Mechanical efficiency	1	Insulation width (mm)	10	Isentropic efficiency	0.85
				Mechanical efficiency	0.85

Table 5.2: Simulation data for the diabatic and adiabatic models.

5.3 A-CAES without TES

The first approach for a small-scale compressed air energy storage plant, was an adiabatic unit. Simulation parameters are presented on Table 5.2. This basic configuration for an A-CAES system was integrated by an isentropic compressor, an insulated steel storage vessel and an isentropic expander. The simplicity of this model was to evaluate the compressed air's potential without adding any heat form. Fig. 5.3 shows the air temperature and pressure variation during charging, storage and discharging times.

First, in the charging time (0 to 45 minutes), the air was compressed from ambient pressure to 15 bar. The air's temperature by the effect of isentropic compression estimated is 388 ^{o}C. So, the vessel will go from 9 bar (minimum vessel's pressure) to 15 bar in about 45 minutes. Besides, the air delivered to the vessel is at 388 ^{o}C, at the end of the charging time, the highest temperature reached in the vessel would be 94 ^{o}C due to heat loss with the surroundings.

Second, during the storage time (45 minutes to 405 minutes), there was a drop in pressure and temperature by the effect of heat loss with the surroundings. After two hours, simulation results on Fig. 5.3 reported that the vessel's pressure will decrease 2 bars and the air's temperature will reach the ambient temperature. The link between pressure lost due to heat loss can be attributed to the energy conservation equations (2.6) and (2.9) explained in Chapter 2.

Third, in the discharging time (405 minutes to 450 minutes), the air will be delivered to the expander at a constant pressure (9 bar) but at variable temperature. During discharging, the air inside the vessels will go from ambient temperature, 15 ^{o}C to -3 ^{o}C. Expander exit temperatures below 3 ^{o}C should be avoided in order to prevent mechanical failures by the effect of precipitate icing [63]. The temperature lost can be attributed to the pressure decrement inside the vessel, again by the effect of the energy conservation equations (2.6) and (2.9). This variation in temperature will lead to a power output variation, therefore, the energy was computed as the integral of the power output during the discharging time. Finally, the air inside the vessel takes 2 hours to reach the initial conditions, in order to start the cycle again. The energy input to run the compressor will be the same for the three simulation models, 1.66kWh. For the A-CAES model without thermal storage the simulated energy output was 0.5 kWh.

5.4 A-CAES with TES

As it was mentioned in Section 2.3, in order to increase the system's efficiency by reducing the energy loss, in this Section is studied the integration of a thermal energy

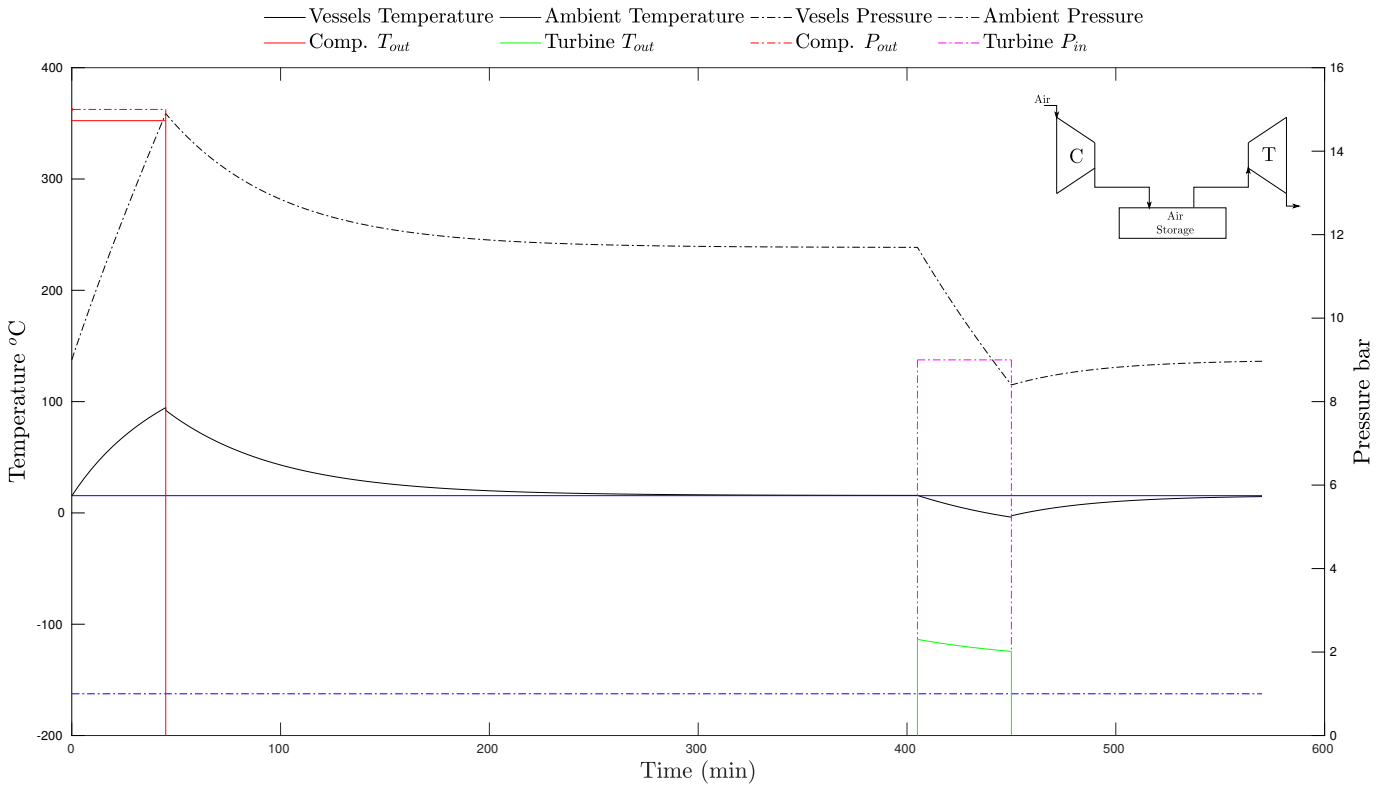

Figure 5.3: Air's pressure and temperature during charging, storage and discharging modes for the A-CAES.

storage unit from the previous adiabatic compressed air energy storage plant. In this way, during the charging time, the heat produced by the compression could be extracted. Then the stored heat could be used to rise the air's temperature during discharging.

Operation parameters were the same listed on Table 5.2. The initial air's temperature T_{gi} at the entry of the packed bed was considered to be the same air's temperature delivered by the compressor 388^{o}C. Additionally, the initial packed bed temperature T_{si} was assumed to be uniform inside the packed bed unit and at ambient temperature (15^{o}C). A packed bed was considered as a thermal energy storage unit according to [6]. Equations (2.12) and (2.13) were approximated by the central differences (5.1) and (5.2) proposed by [64]. Further details about this approximation can be found in the Appendix.

$$\frac{F_g(n+1,i)-F_g(n+1,i-1)}{\Delta y} = -\frac{1}{2}\left[F_g(n+1,i)-F_g(n+1,i-1)\right. \quad (5.1)$$
$$\left. F_s(n+1,i)-F_s(n+1,i-1)\right]$$

$$\frac{F_s(n+1,i)-F_s(n+1,i-1)}{\Delta z} = \frac{1}{2}\left[F_g(n+1,i)-F_g(n+1,i-1)\right. \quad (5.2)$$
$$\left. F_s(n+1,i)-F_s(n+1,i-1)\right]$$

The characteristics of the thermal storage unit are listed on Table 5.3. Adiabatic conditions were assumed for the thermal storage unit, during charging, storage and discharging times. Simulation parameters for the A-CAES unit with thermal storage are shown in Fig. 5.5.

The TES operation can be summarized as follows: first, during charging, the hot air delivered by the compressor go through the TES unit and heat is extracted from the air in each level of the packed bed. Then, the heat extracted from the air is kept until the discharging time. During discharging, the air in the vessel at ambient temperature goes through the packed bed before entering to the expander and heat is extracted from the packed bed to the air.

Parameter	Value	Parameter	Value
T_{gi}	388 ^{o}C	U	0.67 W/(m^2 ^{o}C)
T_{si}	15 ^{o}C	ρ_s	2680 kg/m^3
H	1.2 m	c_s	1068 J
D	0.148 m	υ	0.19537 m/s
ε	0.4	A	180
d	0.02 m		

Table 5.3: Dimensions and operation parameters of the packed bed simulation according to [6]

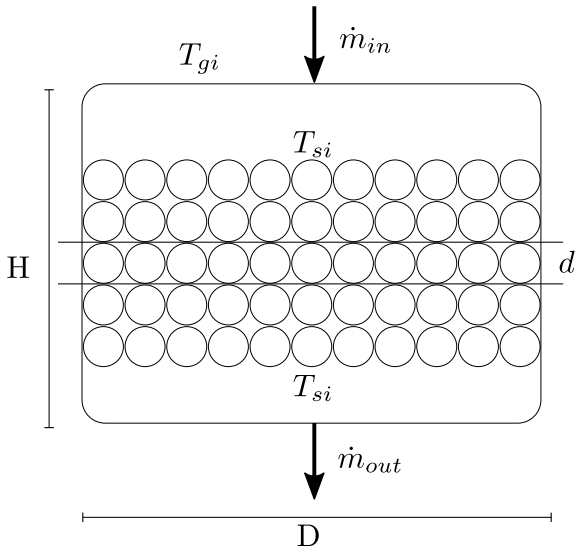

Figure 5.4: Sketch of a packed bed thermal storage system according to [6].

For the A-CAES model with TES, the charging time was similar to the simple A-CAES unit. The compressor delivers air at 15 bar at 388 ^{o}C, then the air goes

through the thermal storage unit, which is at ambient temperature (15^{o}C). At the end of the charging time, the highest temperature in the packed bed will be 95 ^{o}C. Then, the air delivered to the vessel will goes from 143 ^{o}C to 173 ^{o}C. For simplicity, pressure loss in the thermal storage unit were neglected.

During the storage time, the air inside the vessel remain the same as in the simple A-CAES model. In the case of the thermal storage unit, there was not heat loss with the surroundings due to the assumption of adiabatic conditions.

During the discharging time, the air temperature at the exit of the vessels varied from 15 ^{o}C to 3 ^{o}C. But its temperature was risen by the effect of the thermal storage unit, it went from 39 ^{o}C at the beginning of the discharging time to 20 ^{o}C at the end.

The influence of increasing the expander's inlet temperature can be seen in the energy output and round trip efficiency of the CAES model. According to simulation results, the energy output for this model was 0.6 kWh which leads to an increment of 6 % in the round trip efficiency.

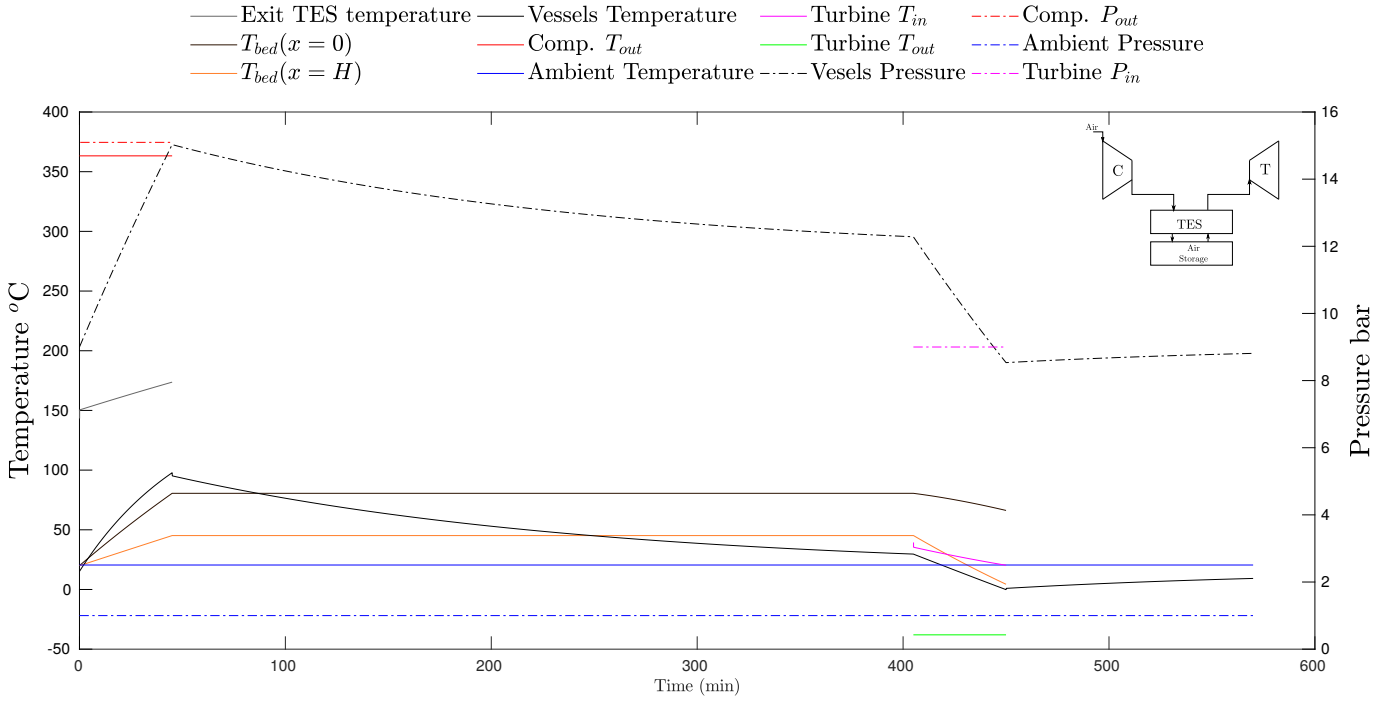

Figure 5.5: Air's pressure and temperature; and packed bed temperature during charging, storage and discharging modes for the A-CAES with thermal storage.

5.5 D-CAES

Lastly, simulation results for the D-CAES model are presented on Fig. 5.6. The D-CAES model considered a combustion chamber in order to rise the air's temperature

to 300 ^{o}C.

For the charging and storage time in the D-CAES model, operation parameters remain the same as in the simple A-CAES model. The difference between the systems relies in the discharging time. During the discharging time, the air temperature is driven to 300 ^{o}C in the combustion chamber. Then, the expander inlet and outlet temperature will be constant as it is shown on Fig. 5.6.

For the D-CAES model, the energy output can be computed just by multiplying the discharging time times the power output. Compared with the simple A-CAES model, the D-CAES model's round trip efficiency was increased 14 % by rising the air's temperature from 15 ^{o}C to 300 ^{o}C.

Furthermore, a constant expander inlet temperature allows the model to be computed in Cycle-Tempo. A simple CycleTempo simulation model is displayed on Fig. 5.7.

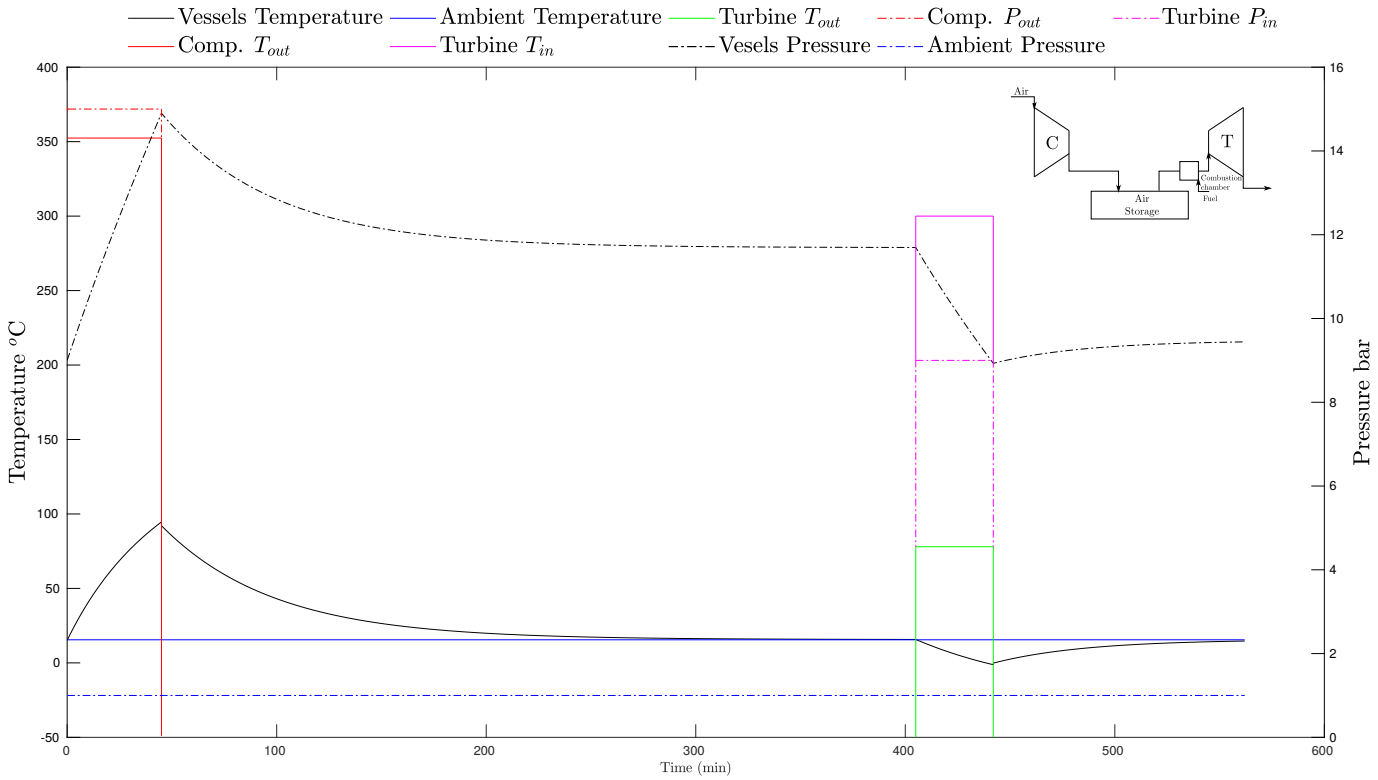

Figure 5.6: Air's pressure and temperature during charging, storage and discharging modes for the D-CAES.

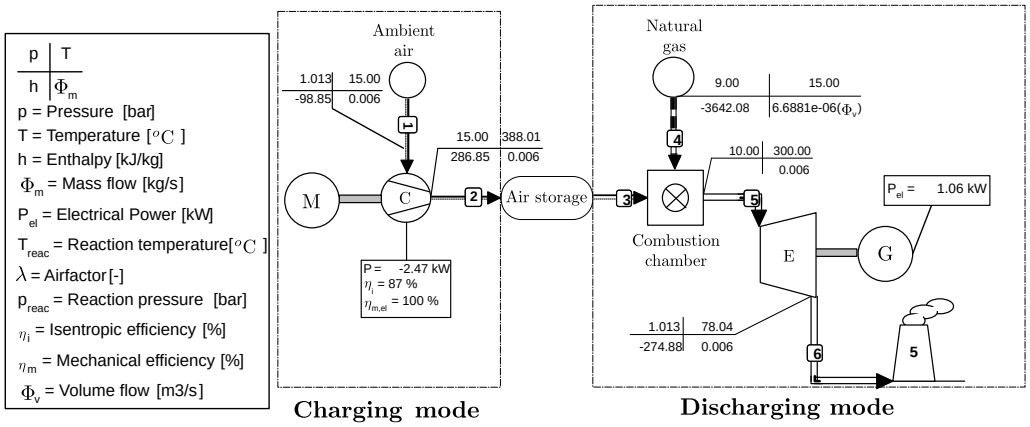

Figure 5.7: D-CAES system's simulation results in CycleTempo.

5.6 Summary

Three compressed air energy storage systems were presented: A-CAES, A-CAES with TES and D-CAES. Table 5.4 provides a summary for each CAES simulation.

Firstly, the A-CAES, is a simple configuration integrated only by the compressor, vessel and expander. Due to heat loss with the surroundings, the turbine exit temperature was below 3 ^{o}C. This exit temperature can cause mechanical failures.

Secondly, the A-CAES with thermal storage. The thermal storage united increased the round trip efficiency from 30% to 36%. The TES unit was able to rise the turbine inlet temperature from ambient temperature (15 ^{o}C) to 39 ^{o}C.

Thirdly, the D-CAES which considered a combustion chamber to rise the expander inlet temperature to 300 ^{o}C increased the round trip efficiency 14%.

Parameter	**A-CAES**	**A-CAES/TES**	**D-CAES**
Energy input (kWh)	1.66	1.66	1.66
Energy output (kWh)	0.5	0.6	0.72
Efficiency (%)	0.3	0.36	0.44
Highest air temperature (^{o}C) after compression	388	388	388
Highest air temperature (^{o}C) after expansion	<3	<15	<78

Table 5.4: Main simulation results for the A-CAES, A-CAES with TES and D-CAES models.

Chapter 6

Varing CAES system initial conditions

In this chapter is studied the effect of varying the initial operation parameters listed on Table 6.1: mass outlet, minimum operation pressure, vessel volume, insulation width, compressor and turbine efficiency. For the following simulation results, when each parameter was varied, the other operation parameters remained constant. Also, according to simulations results reported in the previous chapter, the turbine outlet temperature in the A-CAES goes below -50 ^{o}C. Therefore the following analysis focuses in the D-CAES model which considers a combustion chamber in order to raise the air's temperature before the expansion, see Fig. 5.6.

Parameter	value	Parameter	value	Parameter	value
Charging mode		*Storage*		*Discharging mode*	
Air mas flow rate (kg/s)	0.006	Air storage vessel volume (m^3)	5	Air mas flow rate (kg/s)	0.006
Ambient temperature (^{o}C)	15	Max pressure in vessel (bar)	15	*Expander*	
Compressor		Min pressure in vessel (bar)	9	Inlet pressure (bar)	9
Compression pressure (bar)	15	Heat transfer coefficient (W/(m^2 K))	7.13	Inlet temperature (^{o}C)	300
Isentropic efficiency	0.87	Thermal conductivity (W/(m K))	0.088	(D-CAES only)	
Mechanical efficiency	1	Insulation width (mm)	10	Isentropic efficiency	0.85
				Mechanical efficiency	0.85

Table 6.1: Fixed simulation parameters.

The profit results presented below only considers the energy cost for running the compressor and the energy output per cycle, with a cost-ratio of 4:1, $C_{\text{buy}} = 0.02$ and $C_{\text{sell}} = 0.08\ \frac{Xcurrency}{kWh}$ respectively. The energy cost-ratio 4:1 has been selected as the highest difference between C_{buy} and C_{sell} based on a 24 hours energy cost-cycle presented on Fig. 6.1 based on a day ahead electricity prices [11]. In order to present a general overview of electricity prices the data has been extracted from the *Nord*

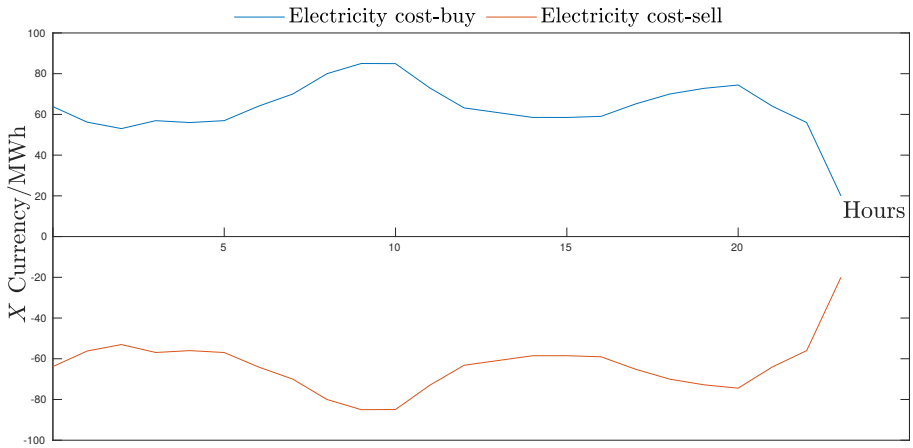

Figure 6.1: Electricity cost-cycle during 24 hours according to the *Nord Pool Group* website [11].

Pool Group website, Nord Pool runs the leading power market in Europe, and they offer day-ahead and intraday markets approximations [65].

The fuel cost in X currency per kWh is considered to be 0.00748 based on the natural gas price reported by [66]. Additionally, the profit analysis presented below, only considers the profit per cycle, it does not consider capital costs or maintenance.

6.1 Mass outlet

First, impact of varying the mass outlet from the vessel which is evaluated. In Chapter 5 the mass outlets from the CAES models was set to 0.006 kg/s. In this Section is evaluated the effect of varying the mass outlet from 0.006 kg/s to 0.024 kg/s. The previous mass outlet flows were considered according to potential discharging times. Simulation results are shown in Figures 6.2 and 6.3.

Figures 6.2 and 6.3 shows that increasing the mass outlet will decrease the discharging times. However, Fig.6.4 shows that there is not a big influence in the profit and energy output. The energy output and profit remains almost constant.

6.2 Vessel's volume

Similarly, the impact of the vessel's volume in the CAES system was evaluated. Fig. 6.5 shows this increment in the energy output for the D-CAES. The increment was stepped due to the Simscape approximation is sensible to the volume increment. As the volume step is reduced, the graphs become smoother. For the purpose of saving computational time, the increment of 1 m^3 was selected.

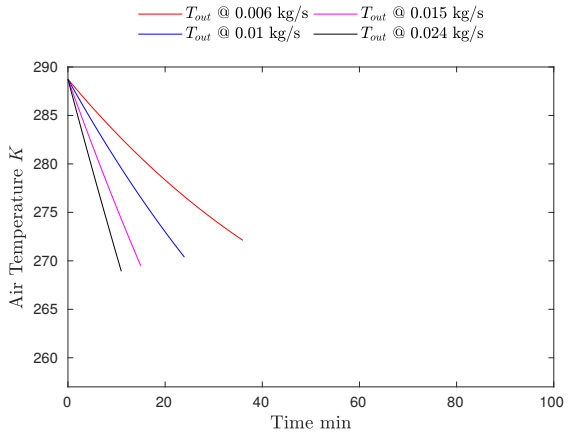

Figure 6.2: Simulated plant temperature in the discharging with different m_{out}.

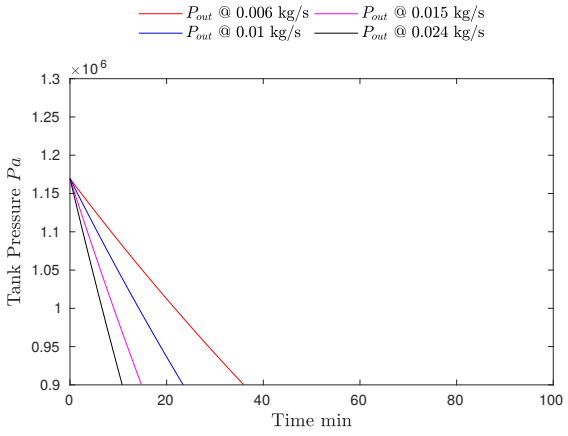

Figure 6.3: Simulated plant pressure in the discharging time with different m_{out}.

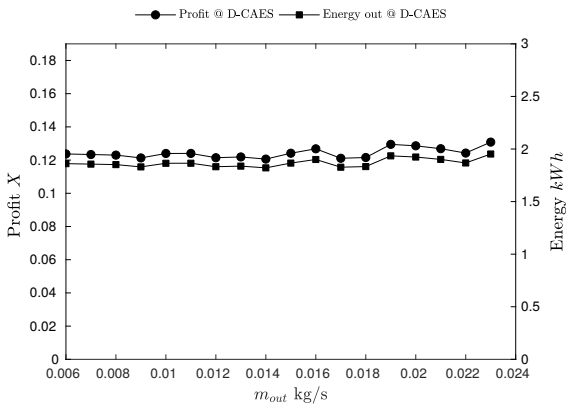

Figure 6.4: D-CAES system's profit and energy output per cycle for different mass outlets.

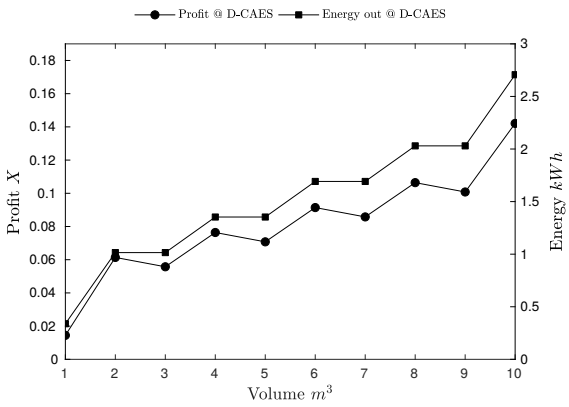

Figure 6.5: D-CAES system's profit and enegy output per cycle for different vessel's volume

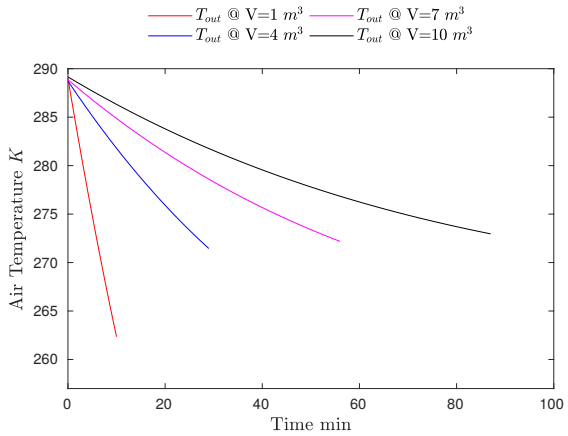

Figure 6.6: Simulated plant's temperature in the discharging with different vessel's volume.

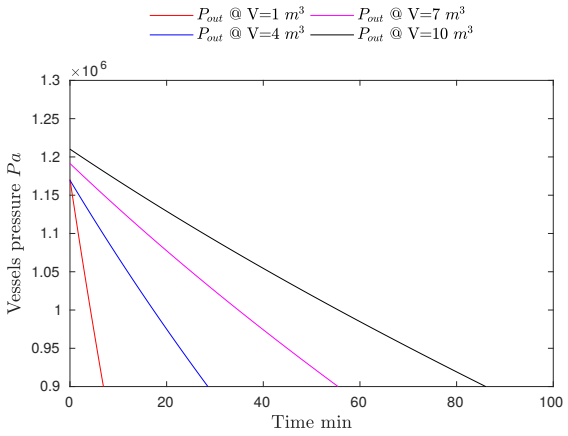

Figure 6.7: Simulated plant's pressure with different vessel's volume.

Figures 6.6 and 6.7 shows the temperature and pressure variation inside the vessel during the discharging time.

From Fig. 6.6 it can be seen that by increasing the vessel's volume, the air's temperature inside the vessel will have less energy losses. Also, this effect in the reduction of temperature loss in the air's inside the vessel can be seen in Fig. 6.2 by decreasing the mass outlet.

It is apparent from Figures 6.6 and 6.7 that bigger vessel's volume will increase the discharging time and the energy output.

6.3 Minimum operation pressure, compressor and turbine efficiencies

The effect of varying the vessel's minimum pressure or the expander working pressure for the D-CAES is shown in Fig. 6.8. From simulation data, the higher the expander inlet pressure the higher the energy output and profit.

From apart of varying the operation parameters presented in the previous section, a brief analysis of the impact of the compressor and expander efficiencies η_c, η_t in the CAES round trip efficiency η_{rt} was done.

Fig. 6.9 shows the effect of varying η_c and η_t from 70 % to 100 % in the round trip efficiency η_{rt}.

As can be seen in Fig. 6.9 the profit per cycle and the round trip efficiency increased by increasing either the compressor efficiency η_c or the expander efficiency η_t. However, it is evident that the expander efficiency has a bigger influence in the CAES performance. This influence, can be observed clearly in the profit gradient for each efficiency, the expander efficiency has a higher profit gradient than the compressor efficiency.

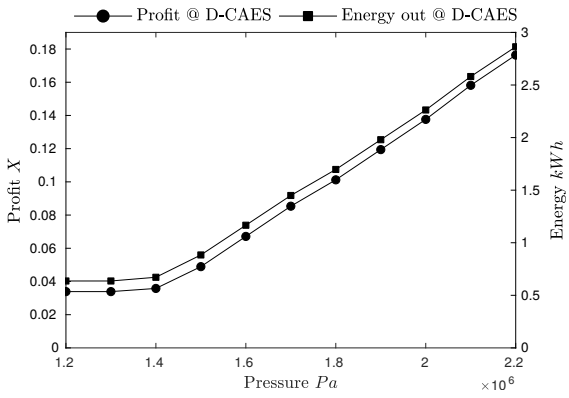

Figure 6.8: D-CAES system's proffit and enegy output for different vessel's minimum pressure

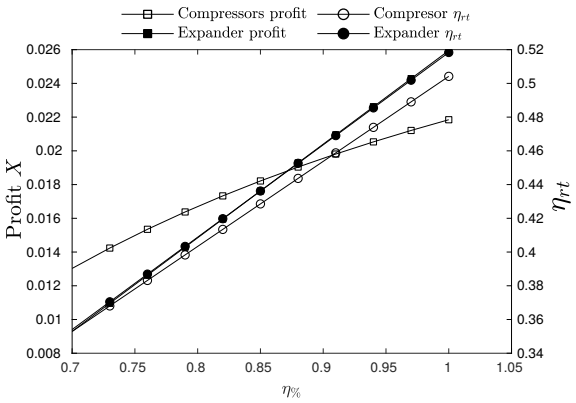

Figure 6.9: Profit per cycle and round trip efficiencies based on different compressor and expander efficiencies, η_c, η_t.

6.4 Insulation width

Fig. 6.10 shows the effect impact of the insulation width I_w in the systems round trip efficiency and profit. Both values, increased when increasing the insulation width. In addition, Fig. 6.11 and 6.12 show the temperature and pressure variation inside the vessel by increasing the default insulation width 10 cm to 80 cm.

The charging, storage and discharging times are kept the same as in the simulation results reported from the previous chapter, 45 minutes during charging and discharging and 6 hours during storage. It is important to consider that the Simscape model simulates the temperature and pressure variation inside the vessels with a constant air temperature and pressure delivering source, it does not consider the physical limit of the compressor if the operation times remains constant. In other words, if air is delivered to the vessel at a given temperature and pressure with constant charging time, it can reached highest pressures inside the vessel in the same charging time when there is less heat loss with the surroundings. Hence, by setting constant operation time while varying the insulation widths I_w it will be reached different pressures and temperatures inside the vessel by the effect of reducing the energy loss by increasing the insulation width.

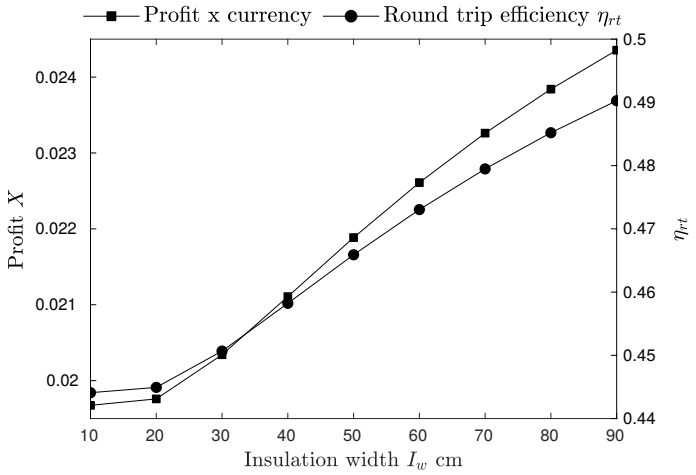

Figure 6.10: D-CAES system's proffit and round-trip efficiency for different insulation widths

Simulation results from Figures. 6.11 and 6.12 can be summarize in the following points.

. During the charging time, it is possible to reach a highest temperature inside the vessel and reach the maximum vessel's pressure in less time.

. During the storage time, there are less heat loss with the surroundings by increasing the insulation width. Also, the air's temperature does not reach the ambient conditions width 40 cm of insulation or more.

. During discharging mode, simulations results show that the air's temperature reduction gradient increases by increasing the insulation width. In other words, there is a higher temperature reduction as a result of the pressure reduction in the vessel by increasing the insulation width. Although, the air reduces its temperature faster, the air's temperature will be delivered to the next component, e.g. TES, combustion chamber, expander; of the operation system at a higher temperature with higher insulation widths if the storage time remains constant.

. Increasing the insulation width will increase the time the vessel takes to reach the initial operation conditions in order to start the cycle again.

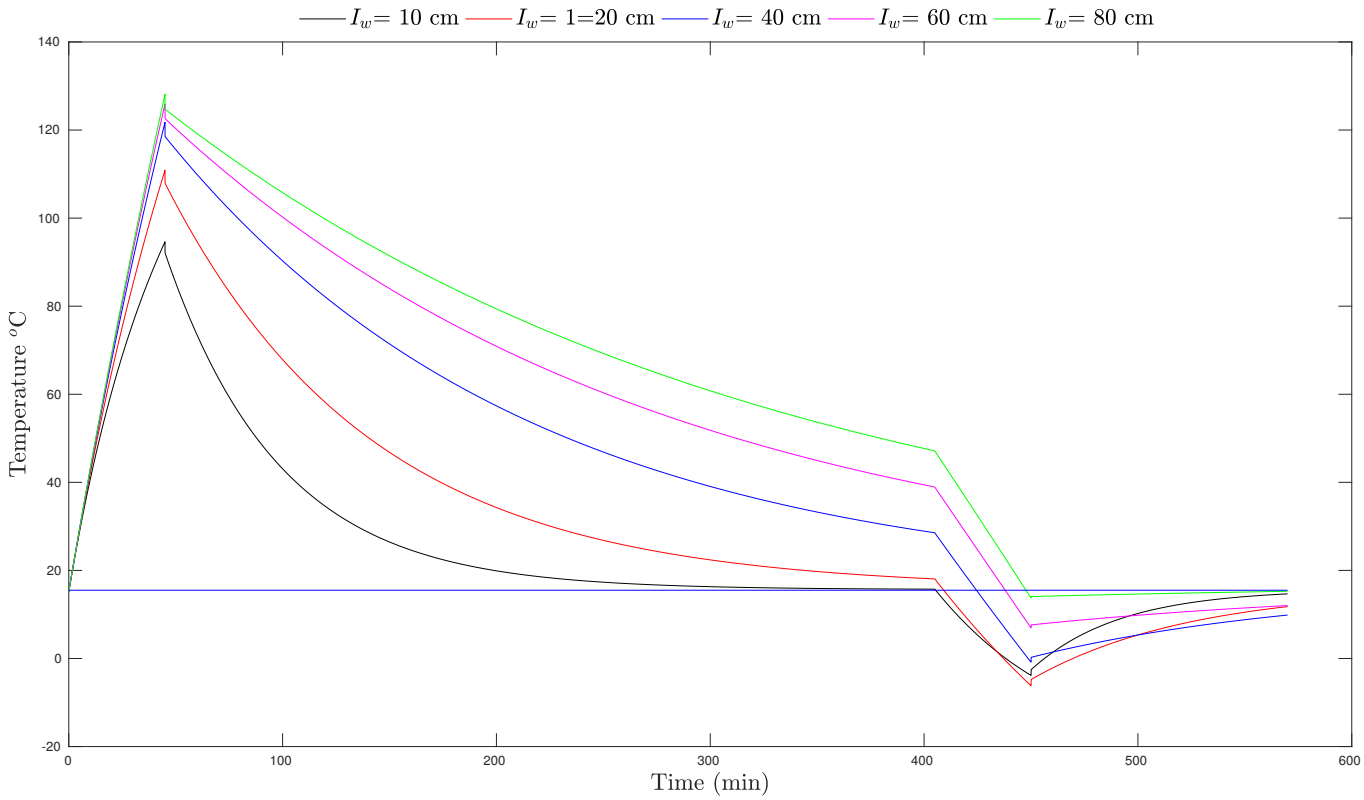

Figure 6.11: Simulated air's temperature inside the vessel during charging, storage and discharging with different insulation widths.

6.5 Summary

To sum up, from this Chapter can be concluded the following about varying the operation parameters.

1. The mass flow rate does not have an impact in the CAES operation.

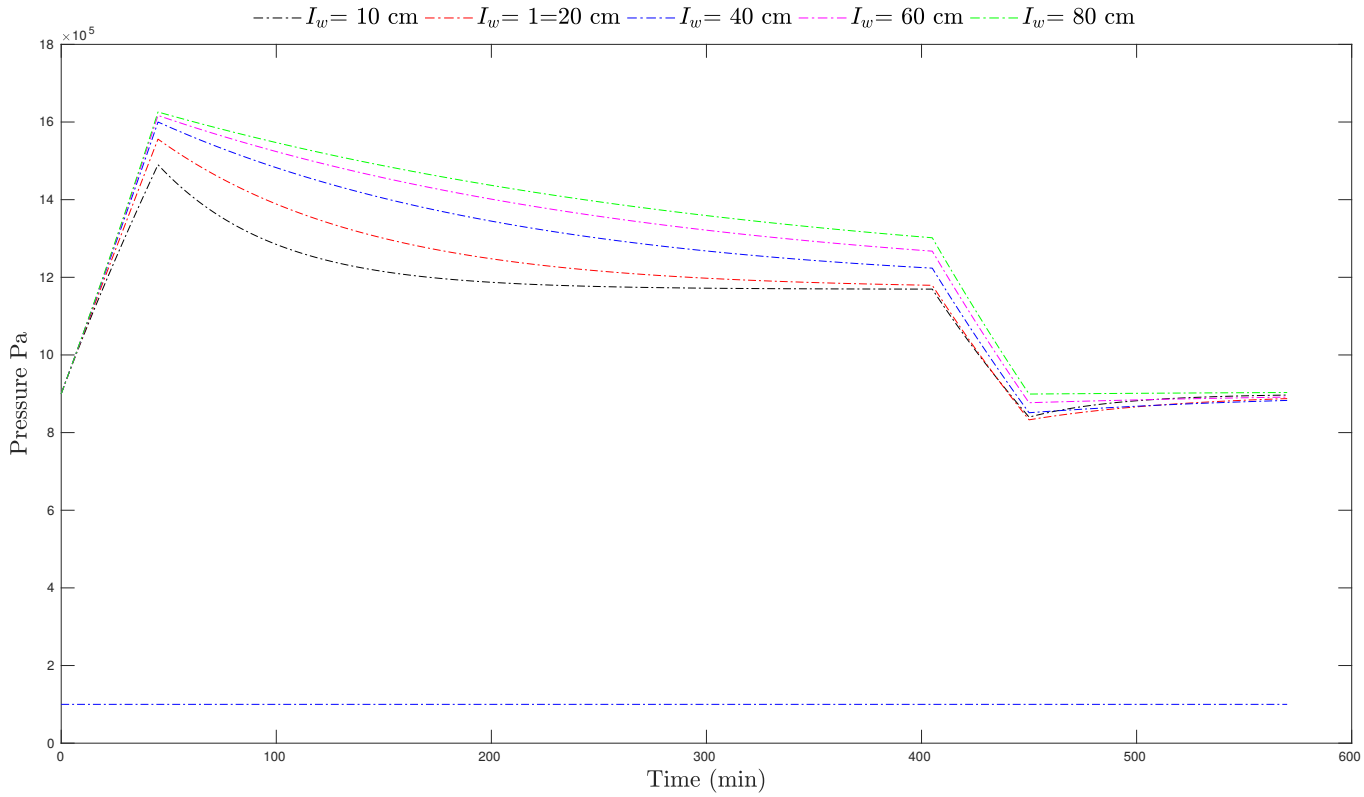

Figure 6.12: Simulated air's pressure inside the vessel during charging, storage and discharging with different insulation widths.

Parameter	**Impact**
Mass flow rate	The profit and energy out remains almost constant.
Vessel's volume	The profit and energy output have a quasi-linear tendency with respect to the vessel's volume.
Minimum operation pressure	Increasing the minimum operation pressure increases the profit and energy output.
Compressor and turbine efficiencies	Although both parameters increase the profit per cycle and the round trip efficiency, the turbine efficiency has a bigger impact in the profit and the round trip efficiency.
Insulation width	The larger the insulation width the less energy loss with the surroundings and the less charging time is required.

Table 6.2: Summary table for the impact of the variation of different operation parameters in the proposed D-CAES system.

2. The vessel's volume has an influence over the energy loss. Bigger vessel's volumes will reduce the air's temperature decrement during expansion. Additionally, it is increased the profit per cycle with bigger vessel's volumes.

3. Increasing the minimum operation pressure is the parameter with the higher influence in the system profit. Just by increasing the minimum operation pressure from 12 bar to 22 bar, it is possible to get the same profit per cycle as by increasing the vessel volume to 10 m^3.
4. The expander has a higher influence in the round trip efficiency rather than the compressor.

Finally, from the data presented above can be recommended to increase the insulation width and select the compressor and expander with the highest efficiency. Also, it is evident the need to design a CAES system with the highest minimum operation pressure and vessel's volume according to the ability of the operation conditions in order to maximize the plant profitability.

Chapter 7

D-CAES and Batteries η_{rt}

In order to compare the small-scaled D-CAES system explained before, which was the most reliable CAES model based on simulation results presented in Chapter 5, 4 energy storage systems were considered: pump-heat energy storage, pump-hydro energy storage, hydrogen energy storage and a 3.3 kWh lithium-battery. The system's parameters listed on Table 7.1 are explained below:

Round trip efficiency η_{rt} of each system. Which is a relationship of the energy output and energy input for the storage system. In other words, it is the ratio of energy put in to energy retrieved from storage. This measure provides information about how efficient is the system.

Life cycle. Results presented on Table 7.1 are the expected operation life of each system.

Profit per cycle. The profit per cycle has been computed considering the same energy input computed to operate the D-CAES system $E_{in} = 1.6$ kWh and with each round trip efficiency the energy output was approximated for each system. Then with a cost ratio of 4:1 from Chapter 6 the profit per cycle was computed.

Capital cost/KWh. The capital cost considered exclusively the cost of each system component to start the operation according to each reference, it did not consider any operation or maintenance cost.

From Table 7.1 it can be pointed out the following points for the proposed D-CAES system compared with other energy storage systems

. The D-CAES life cycle is larger than the other technologies. Compared with the lithium-battery it is 3.75 times longer.

. Compared with other technologies, the D-CAES system has a lower efficiency and profit per-cycle.

	D-CAES	3.3 kWh L-Battery	Pump heat ES	Pump-hydro ES	Hydrogen ES
η_{rt}	0.44	0.95	0.72	0.88	0.58
Life cycle (years)	30	8	20	20	26
Profit per cycle (X currency)	0.0271	0.093	0.06	0.084	0.0422
Capital cost/kWh	24795	3840	918	366.14	434
Reference	-	[67]	[68]	[69]	[70]

Table 7.1: Main system's parameters for the D-CAES and other energy storage technologies.

. Considering the off-the-shelf components from Fig. 5.1, the D-CAES has a higher capital cost per energy output.

7.1 Net present value analysis

The net present value (NPV) analysis is a simple approach to evaluate the value of money over a period of time in order to estimate project's probability based on initial investments and cash flows over a period of time.

It was computed the NPV of the D-CAES system and compared with batteries. For the annual profit the plant was assumed to operate 2 times a day every day of the year (365 days) for 25 years. Additionally, it was excluded any maintenance cost. However, in the case of batteries, initial investment every 8 years was considered, according to their life cycle. Investments and cash flow for each system are presented in Fig. 7.1.

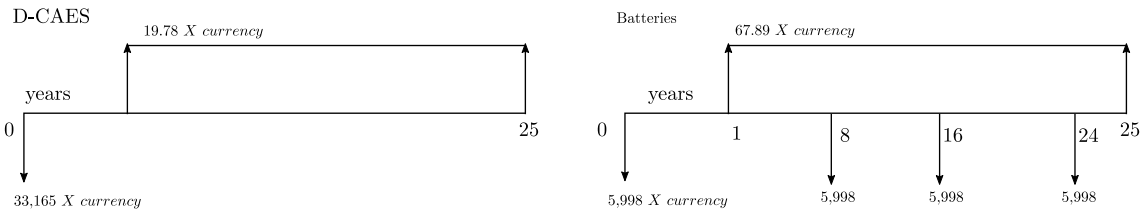

Figure 7.1: Net present value analysis for 25 years for the D-CAES and batteries.

NPV_{CAES}=-32,985 *X currency*.
$\text{NPV}_{Batteries}$=-7459.6 *X currency*.

The existing energy returned on energy invested (EROEI) and the energy cost ratio were insufficient to make the operation of a CAES or batteries systems profitable for 25 years.

For both systems it is evident the high capital cost. In order to make any system profitable, the net present value of the system's profit per year $\text{NPV}_{\text{profit-year}}$, should be higher than the capital cost:

$$\text{NPV}_{\text{profit-year}} >> \text{Investment}$$

So considering the electricity cost ratio 4:1, in order to make the CAES system profitable, the capital cost should be lower than 180 in X currency.

Chapter 8

Discussion

This study was set out with the aim of assessing the potential of small-scaled Compressed Air Energy Storage. Due to the ongoing integration of renewable energy sources, the idea of small-scaled energy storage was explored. In this work, small-scaled referred to a system that can be fit in any available space in a house, e.g a garage.

Prior studies have noted the importance of energy storage and have proposed multiple multimega-watts energy systems [16,20,22]. However, very little was found in literature on the question of the potential of Small-scaled Compressed Air Energy Storage. To answer this, a thermodynamic and economical approach was proposed for the assessment of a s-c CAES based on off-the-shelf components easily available on the market.

Two thermodynamic models were developed for the CAES systems evaluation. On the one hand, the steady approach made with cycle tempo gave a general overview of the system when most of the operation data was available. On the other hand the unsteady approach allowed the complete design and operation analysis of the CAES systems from scratch. The main strength of the unsteady approach for this work was the ability to compute operation times. In addition, the model built in Simscape was validated when it was simulated and compared with the experiment carried by Venkataramani et al. [4]. The percentage of error computed was 0.39%, with two significant digits of confidence, it provided confidence to run CAES simulations. Although the Simscape's model accuracy was not studied, from simulation results computed on Chapter 6, smoother graphs where observed when the simulation pace was smaller.

Furthermore, 3 CAES systems were evaluated: simple A-CAES, A-CAES with thermal storage and D-CAES.

Firstly, the main motivation to study a simple A-CAES system, integrated exclusively by the compressor, insulated vessel and expander, was that the insulated

vessel was going to be able to keep the air's temperature (388 °C) after the compression, then use the air to drive the expander. The results of this experiment indicated that due to energy losses with the surroundings, the air reached the ambient temperature after two hours, this produced turbine exit temperature lower than -50 °C, which makes the system operation unfeasible with this configuration.

Secondly, the integration of a thermal storage system was considered in order to preserve the air's temperature after compression. A simple form of TES was selected: a packed bed. For simplicity, it was considered to be a perfect insulated TES. Although the highest temperature at the entry of the packed bed reached was 95 °C, the highest air's temperature at the exit of the packed bed during discharging, 39°C, was insufficient to rise the turbine inlet temperature enough to avoid temperatures below -10 °C. Contrary to expectation, the integration of a TES unit did not provide a significant impact on the system. However, these simulation results further support the claims often found in literature: higher round trip efficiencies are reported when the adiabatic systems operates with higher pressures e.g. 42 bar [9]. This can be explained by the fact that higher compressed ratios provide higher air temperatures after compression. Nonetheless, the 15 bar operation pressure was considered in this study due to the compressor cost, size and availability on the market. Higher operation pressures will require more sophisticated and bigger components, so the concept of small-scaled system might be lost.

Thirdly, a combustion chamber was included in order to raise the turbine inlet temperature, therefore the D-CAES model was evaluated.

In accordance with the present results reported, the most profitable with the highest round trip efficiency s-c CAES approach was a D-CAES. Based on the proposed simulation parameters, an A-CAES was not profitable due to the heat loss with its surroundings. Even with the addition of a TES, the mass flow rate was not high enough to provide an efficient heat transfer process. Table 8.1 provides a summary of the round trip efficiency for each system.

Parameter	**A-CAES**	**A-CAES/TES**	**D-CAES**
Energy input (kWh)	1.66	1.66	1.66
Energy output (kWh)	0.5	0.6	0.72
Efficiency (%)	0.3	0.36	0.44

Table 8.1: Energy input , energy output and efficiency of the A-CAES, A-CAES with TES and D-CAES models.

Furthermore, prior studies have reported higher efficiencies for large scale CAES

systems (up to 100 MW) [9, 71, 43]. For small work densities, 1kW to 5 kW, the existing off-the-shelf components for CAES systems made them uncompetitive with batteries. Due to two main points: capital cost and round trip efficiency.

Capital cost. In economic terms, the s-c D-CAES was unprofitable mainly for its capital cost. The proposed s-c D-CAES system capital cost is 4 times higher than Lithium-battery storage. The high capital cost was attributed to the off-the-shelf components, especially to the expander and the iron vessel.

Round trip efficiency. The reported round trip efficiency for the proposed s-c CAES unit was 44 %. From Chapter 6, higher round trip efficiencies were achieved when increasing the expander efficiency, the minimum operation pressure and the storage capacity.

On the other hand, in order to make the system viable, the following considerations are proposed:

1. *Capital cost and system profit.* The capital cost of the CAES system should be lower than the system probability during its life cycle. In other words the capital cost should be lower than the net present value of the system profit. Designing and manufacturing a expander in mass could reduce capital cost by 30 % [72].

2. *Storage capacity.* The capital cost could be reduced 30 % by changing the storage facility for a cavern. Also, higher round trip efficiencies are reported when caverns are used for the storage facility [10].

3. *High compression ratios.* From Chapter 6, higher efficiencies were achieved when increasing the minimum operation pressure. For example, Kim and Favrat [73] simulated CAES systems with 50 bar minimum pressure and they reported efficiencies up to 74%.

4. *Component's design.* Designing appropriate components for the s-c CAES is crucial to improve the CAES profitability and round trip efficiency. For example, [74] proposed a radial-inflow expander configuration for a small scaled CAES, whilst [75] studied a quasi-isothermal expander and [3] presented an expander selection review.

5. *Free input energy.* If we considered using subsidies or existing small-scaled renewable energy production, then the cost of the energy input to run the CAES system could be neglected and the system profitability could increase up to 40%.

Finally, CAES systems built with off-the-shelf components are not profitable for small work densities (1kW to 5kW), other storage system should be considered based on the energy demand. However, small-scaled compressed air energy storage is a profitable storage system when the capital cost is lower than the net present value of the system profit. This could be achieved with the integration of second-hand off-the-shelf components like the experiment carried out by Venkataramani et al. [4] or government subsidies. Additionally, CAES can be used to avoid shut-down plant's cost. For example, in 2018 Britain's wind farms were paid £100 million to not produce electricity because at certain times Britain's electricity network is unable to cope with the power they produce [76]. In this context, the money invested to shut-down the wind farms could be spent on installing CAES systems, then wind farms would be able to store the energy produced and costs for shut-down could be eliminated.

Chapter 9

Conclusions

9.1 General conclusions

◇ A literature review has been done. It points out the following points:

  · The role of energy storage related to renewable energies.

  · The outstanding electrical energy storage systems.

  · The operation of a compressed air energy storage plant and different configurations (D-CAES, A-CAES and I-CAES).

  · The research done in small-scaled CAES.

  · The role of small-scaled compressed air energy storage in the decentralization of electrical energy

◇ The vessel's size can be considered as the main parameter for the compressed air energy storage design in this research. Considering that this design is meant to be fit into a garage or a basement, the vessel's size would be one of the main system's boundaries.

◇ The first CAES approach was an steady model in Cycle-Tempo. Cycle-Tempo was useful to start sizing and study the system. It helped to state the initial operation parameters for a small-scaled plant. Also, by simulating different operation parameters it was possible to identify potential components (e.g. compressor, expander and vessel's size) and estimate energy inputs and outputs.

◇ Cycle tempo can be used only when the expander's inlet temperature is constant and the operation times are known. So it is only suitable to estimate the compressor energy input and the expanders energy output and the fuel consumption. But still, operation times are computed with simscape.

- ◇ The second CAES approach was a dynamic model in Matlab/Simscape. The dynamic model was built based on the operation parameters from the steady model. With this new approach, it was possible to compute operation times. Also, it helped to analyse different energy loses during storage and expansion. Furthermore, it provided an understanding of the air's properties inside the vessel at different stages.

- ◇ Based on the steady and dynamic approaches. The potential of a Small-scaled Compressed Air Energy storage plant has been evaluated. Three different CAES models have been simulated, a simple A-CAES, an A-CAES with thermal storage and a D-CAES.

- ◇ Due to an air's temperature decrement inside the vessel by the effect of a pressure reduction during the discharging mode, the most suitable CAES system is the diabatic one.

- ◇ Adding a simple thermal storage unit leads to an increment of 6 % in the round trip efficiency of the simple A-CAES model.

- ◇ The price of energy can be crucial to make profitable a s-c CAES system . It would determine the proper operating times for the CAES unit.

- ◇ Expanders for compressed air energy storage plants has to investigated in order to increased the system efficiency, it should be considered a proper expander based on the system operation parameters.

- ◇ Further studies will determine the optimal operation parameters, e.g. inlet and outlet mass flow, insulation width, minimum operation pressure, etc.

9.2 Future work

The following points are suggested for future studies in small-scaled compressed air energy storage.

. Consider the effect of heat losses with the surroundings for the operation pressure.

. It should be taken into account to consider the optimum insulation width according to the vessel's volume when using a vessel as the storage facility.

. Find the optimum operation conditions based on the CAES system type.

. Find a suitable thermal storage unit based on the operation parameters for the CAES system, either for the A-CAES or the D-CAES

. Design a expander according to the operation parameters could decrease the capital cost and increase the round trip efficiency.

. Design the control system to operate the CAES plant.

Appendix

Matlab script

```
%%  Script to compute the Sc-CAES with fixed values
%   Ta       Ambient temperature C
%   Pa       Atmospheric pressure bar
%   mf       Mass flor rate inlet kg/s
%   mf_out   Mass flow rate outlet kg/s
%   V        Vessel Volume m3
%   l_v      Vessel Length m
%   A        Vessel area m2
%   P_v      Maximum vessel pressure Pa
%   P_in     Vessel Intial Vessel's Pressure bar charging
   mode
%   T_in     Vessel Intial Vessel's Temperature  charging
   mode C
%   T_inS    Vessel initial temperature in store mode K
%   P_inDis Vessel initial pressure in discharging mode
   Pa
%   T_inDis Vessel initial Temperature in discharging
   mode K
%   P_dis    Vessel outlet pressure at constant outlet
   flow Pa
%   T_dis
%   t        Charging time min
%   t2       Store time h
%   t3       Discharging time min
%   k        Isentropic Exponent
```

```
%   R        Specific gas constant kJ/(kg K)
%   Po        Power kW
%   Po_av     Average power output
%   E_       Energy kWh
%   L_out    Cost of selleing the energy Pounds/kWh
%   L_in     Cost of buying the energy to drive the
   compressor Pounds/kWh
%  Profit    Profit X currency
      %% Initial Parameters
Ta=15; Pa=1; mf=0.006; P_in=9; T_in=15;  P_v=15e5;
V=5; i=0; l_v=4.26; thickness=.5;
A_v=2*V/l_v+2*sqrt(pi*V*l_v);mf=0.006;  mf_out=0.006;
   mf_s=0;
k=1.4; R=0.287101;t=60*45; t2=60*60*6; t3=60*45;  t4
   =60*60*2;
     %% Charging mode
    sim('ScCharging'); %Simscape charging model
     %% Storage mode
    T_inS=T_ch(end); P_inS=P_ch(end);
    sim('ScStorage'); %Simscape storage model
    tv1=t_char; %Vector time charging mode
    tv2=t_char(end)+t_s; %Vector time storage mode;
    %% Discharging mode %Simscape discharging model
     P_inDis=P_s(end); T_inDis=T_s(end);
    sim('ScDischarging');
    tv3=tv2(end)+t_dis;
     %% Cycle end       %Simscape resting model
    T_inS=T_dis(end); P_inS=P_dis(end);
    sim('ScStorage2');
    tv4=tv3(end)+t_s2;
     %% Power-Energy
    v1=1/airProp2(T_in+273, 'rho'); %Specific Volume
    Po_in=mf*v1*1e5*k/(k-1)*(15^((k-1)/k)-1)*.85/1000;
    P_out=mf_out*k/(k-1)*R.*(T_dis).*(1-(1e5./8e5)^((k-1)
       /k));
    E_in=t/60/60*Po_in;
    E_out=trapz(t_dis,P_out)/3600; %kWs-> kJ || kWs/60->
       kW min || kW min/60-> kWh
```

TES Numerical method

The numerical method to compute the thermal storage model described in Chapter 2 is described below.

According to [56] equations (2.12) and (2.13) can be dimensionless by transforming the independent variables x and t,

$$\begin{aligned} y &= \alpha_2 \frac{x}{\upsilon} \\ z &= \alpha_1 \left(t - \frac{x}{\upsilon} \right) \end{aligned}$$

and introducing the following normalized temperatures

$$F_s = \frac{T_s - T_{si}}{T_{gi} - T_{si}} \qquad F_g = \frac{T_g - T_{gi}}{T_{gi} - T_{si}}$$

the dimensionless form of the thermal storage model from Chapter 2 will be,

$$\frac{\partial F_g}{\partial y} = -(F_g - F_s) \tag{9.1}$$

$$\frac{\partial F_s}{\partial z} = F_g - F_s \tag{9.2}$$

with the initial conditions

$$F_g(y,0) = e^{-y} \qquad F_s(y,0) = 0$$

and the boundary conditions,

$$F_g(0,z) = 1 \qquad F_s(0,z) = 1 - e^{-(z + \alpha_1 \frac{H}{\upsilon})}$$

Equations 9.1 and (9.2) can be approximated by a central difference formula [64], for the computational domain,

$$\begin{aligned} \frac{F_g(n+1,i) - F_g(n+1,i-1)}{\Delta y} &= -\frac{1}{2} [F_g(n+1,i) - F_g(n+1,i-1) \\ &\quad F_s(n+1,i) - F_s(n+1,i-1)] \\ \frac{F_s(n+1,i) - F_s(n+1,i-1)}{\Delta z} &= \frac{1}{2} [F_g(n+1,i) - F_g(n+1,i-1) \\ &\quad F_s(n+1,i) - F_s(n+1,i-1)] \end{aligned}$$

Therefore, for each node the system of equations will be:

$$\begin{bmatrix} 2+\Delta y & -\Delta y \\ -\Delta z & 2+\Delta z \end{bmatrix} \begin{bmatrix} F_g[n+1,i] \\ F_s[n+1,i] \end{bmatrix} = \begin{bmatrix} (2+\Delta y)F_g[n+1,i-1] + \Delta y F_s[n+1,i-1] \\ \Delta F_g[n,i] + (2-\Delta z) + (2-\Delta z)F_s[n,i] \end{bmatrix}$$

Bibliography

[1] Ryan Elliman, Christopher Gould, and Moofik Al-Tai. Review of current and future electrical energy storage devices. *2015 50th International Universities Power Engineering Conference (UPEC).*

[2] Ioan Sarbu and Dand Calin Sebarchievici. A comprehensive review of thermal energy storage. *Sustainability*, 10(2):191, jan 2018.

[3] Wei He and Jihong Wang. Optimal selection of air expansion machine in compressed air energy storage: A review. *Renewable and Sustainable Energy Reviews*, 87:77 – 95, 2018.

[4] Gayathri Venkataramani, E. Ramakrishnan, Mangat Ram Sharma, A. Hari Bhaskaran, Prabir Kumar Dash, Velraj Ramalingam, and Jihong Wang. Experimental investigation on small capacity compressed air energy storage towards efficient utilization of renewable sources. *Journal of Energy Storage*, 20:364 – 370, 2018.

[5] Atlas-Copco. Oil-injected compressors catalogue.

[6] A. Elouali, T. Kousksou, T. El Rhafiki, S. Hamdaoui, M. Mahdaoui, A. Allouhi, and Y. Zeraouli. Physical models for packed bed: Sensible heat storage systems. *Journal of Energy Storage*, 23:69 – 78, 2019.

[7] Daniel Wolf and Marcus Budt. Lta-caes – a low-temperature approach to adiabatic compressed air energy storage. *Applied Energy*, 125:158–164, July 2014.

[8] Guruprasad Alva, Yaxue Lin, and Guiyin Fang. An overview of thermal energy storage systems. *Energy*, 144:341 – 378, 2018.

[9] Marcus Budt, Daniel Wolf, Roland Span, and Jinyue Yan. A review on compressed air energy storage: Basic principles, past milestones and recent developments. *Applied Energy*, 170:250 – 268, 2016.

[10] Wei He, Xing Luo, David Evans, Jonathan Busby, Seamus Garvey, Daniel Parkes, and Jihong Wang. Exergy storage of compressed air in cavern and

cavern volume estimation of the large-scale compressed air energy storage system. *Applied Energy*, 208:745–757, December 2017.

[11] https://www.nordpoolgroup.com/market-data1/gb/auction-prices/uk/hourly/?view=table.

[12] Vaclav Smil. *Energy in world history*. Essays in world history. Westview Press, Boulder, 1994.

[13] Phebe Asantewaa Owusu and Samuel Asumadu-Sarkodie. A review of renewable energy sources, sustainability issues and climate change mitigation. *Cogent Engineering*, 3(1), December 2016.

[14] Felix Cebulla, Jannik Haas, Josh Eichman, Wolfgang Nowak, and Pierluigi Mancarella. How much electrical energy storage do we need? a synthesis for the u.s., europe, and germany. *Journal of Cleaner Production*, 181:449–459, April 2018.

[15] David Elliott. *Renewables : a review of sustainable energy supply options*. 2013.

[16] OFGEM. State of the energy market 2019 report. Technical report, The Office of Gas and Electricity Markets, 2019.

[17] BEIS. The uks draft integrated national energy and climate plan (necp). Technical report, Department of Business, Energy and Industrial Strategy, 2019.

[18] "towards a new energy strategy". https://ec.europa.eu/energy/en/consultations/towards-new-energy-strategy-europe-2011-2011. Accessed: 20-03-2018.

[19] D. Pimentel, G. Rodrigues, T. Wang, R. Abrams, K. Goldberg, H. Staecker, E. Ma, L. Brueckner, L. Trovato, and C. Chow. Renewable energy: Economic and environmental issues. *Bioscience*, 44(8), 1994.

[20] Andrew D. Mills, Todd Levin, Ryan Wiser, Joachim Seel, and Audun Botterud. Impacts of variable renewable energy on wholesale markets and generating assets in the united states: A review of expectations and evidence. *Renewable and Sustainable Energy Reviews*, 120:109670, mar 2020.

[21] Souvik Sen and Sourav Ganguly. Opportunities, barriers and issues with renewable energy development – a discussion. *Renewable and Sustainable Energy Reviews*, 69:1170–1181, March 2017.

[22] DAVID Pimentel, MEGAN HERZ, MICHELE GLICKSTEIN, MATHEW ZIMMERMAN, RICHARD ALLEN, KATRINA BECKER, JEFF EVANS,

BENITA HUSSAIN, RYAN SARSFELD, ANAT GROSFELD, and THOMAS SEIDEL. Renewable energy: Current and potential issues. renewable energy technologies could, if developed and implemented, provide nearly 50energy needs; this would require about 17 *BioScience*, 52(12):1111–1120, December 2002.

[23] Frank S. Barnes and Jonah G. Levine. *Large energy storage systems handbook*. Mechanical engineering series (Boca Raton, Fla.). CRC Press, Boca Raton, Fla. ; London, 2011.

[24] Andreas Belderbos, Ana Virag, William D'haeseleer, and Erik Delarue. Considerations on the need for electricity storage requirements: Power versus energy. *Energy Conversion and Management*, 143:137–149, July 2017.

[25] Karni Siraganyan, Dasaraden Mauree, A. T. D. Perera, and Jean Louis Scartezzini. Evaluating the need for energy storage to enhance autonomy of neighborhoods. 2017.

[26] Nathan Lewis. Research opportunities to advance solar energy utilization. *Science*, 351(6271), January 2016.

[27] David Parra, Maciej Swierczynski, Daniel I. Stroe, Stuart.A. Norman, Andreas Abdon, Jörg Worlitschek, Travis O'Doherty, Lucelia Rodrigues, Mark Gillott, Xiaojin Zhang, Christian Bauer, and Martin K. Patel. An interdisciplinary review of energy storage for communities: Challenges and perspectives. *Renewable and Sustainable Energy Reviews*, 79:730 – 749, 2017.

[28] J. Eyer and G. Corey. Energy storage for the electricity grid: Benefits and market potential assessment guide. pages 1–232, 01 2011.

[29] Bert Droste-Franke. Review of the need for storage capacity depending on the share of renewable energies. In *Electrochemical Energy Storage for Renewable Sources and Grid Balancing*, pages 61–86. Elsevier, 2015.

[30] Mike Quashie, Chris Marnay, François Bouffard, and Géza Joós. Optimal planning of microgrid power and operating reserve capacity. *Applied Energy*, 210:1229–1236, jan 2018.

[31] A. (Andrei) Ter-Gazarian. *Energy storage for power systems*. IEE energy series ; 6. Peter Peregrinus on behalf of the Institution of Electrical Engineers, Stevenage, 1994.

[32] Mathew Aneke and Meihong Wang. Energy storage technologies and real life applications – a state of the art review. *Applied Energy*, 179:350 – 377, 2016.

[33] Ashim Gurung and Qiquan Qiao. Solar charging batteries: Advances, challenges, and opportunities. *Joule*, 2018.

[34] John R. Miller. Perspective on electrochemical capacitor energy storage. *Applied Surface Science*, 460:3 – 7, 2018. Advanced functional materials for supercapacitors.

[35] Paul Breeze. Chapter 5 - superconducting magnetic energy storage. In Paul Breeze, editor, *Power System Energy Storage Technologies*, pages 47 – 52. Academic Press, 2018.

[36] Ayse Selin Kocaman and Vijay Modi. Value of pumped hydro storage in a hybrid energy generation and allocation system. *Applied Energy*, 205:1202 – 1215, 2017.

[37] Mehdi Mehrpooya, Bahram Ghorbani, and Seyed Sina Hosseini. Thermodynamic and economic evaluation of a novel concentrated solar power system integrated with absorption refrigeration and desalination cycles. *Energy Conversion and Management*, 175:337 – 356, 2018.

[38] Dennis Kreid. Analysis of advanced compressed air energy storage concepts. Technical report, U.S. Department of Energy under Contract EY-76-C-061830, October 1977.

[39] R. W. (Richard Wilson) Haywood. *Analysis of engineering cycles : power, refrigerating and gas liquefaction plant.* Pergamon, Oxford, 4th ed. edition, 1991.

[40] D. Wolf. Methods for design and application of adiabatic compressed air energy storage based on dynamic modeling, 2011.

[41] M. Nakhamkin, L. Andersson, E. Swensen, J. Howard, R. Meyer, R. Schainker, R. Pollak, and B. Mehta. Aec 110 mw caes plant: Status of project. *Journal of Engineering for Gas Turbines and Power*, October 1992.

[42] Xing Luo, Jihong Wang, Mark Dooner, Jonathan Clarke, and Christopher Krupke. Overview of current development in compressed air energy storage technology. *Energy Procedia*, 62:603–611, 2014.

[43] Chao Qin and Eric Loth. Liquid piston compression efficiency with droplet heat transfer. *Applied Energy*, 114:539 – 550, 2014.

[44] E. Jannelli, M. Minutillo, A. Lubrano Lavadera, and G. Falcucci. A small-scale caes (compressed air energy storage) system for stand-alone renewable energy

power plant for a radio base station: A sizing-design methodology. *Energy*, 78:313–322, December 2014.

[45] Alexandru Ciocan, Mohand Tazerout, Tudor Prisecaru, and Jean-Felix Durastanti. Thermodynamic evaluation for a small scale compressed air energy storage system by integrating renewable energy sources. pages 455–460. IEEE, November 2015.

[46] "sustainx isothermal compressed air energy storage". https://www.energy.gov/sites/prod/files/SustainX.pdf, 2010. Accessed: 02-04-2018.

[47] Sunil Luthra, Sanjay Kumar, Dixit Garg, and Abid Haleem. Barriers to renewable/sustainable energy technologies adoption: Indian perspective. *Renewable and Sustainable Energy Reviews*, 41:762–776, jan 2015.

[48] Evanthie Michalena and Jeremy Hills. Renewable energy issues and implementation of european energy policy: The missing generation? *Energy Policy*, 45:201–216, 2012.

[49] Karoly Nagy and Krisztina Körmendi. Use of renewable energy sources in light of the "new energy strategy for europe 2011–2020". *Applied Energy*, 96:393–399, aug 2012.

[50] Kaoshan Dai, Anthony Bergot, Chao Liang, Wei-Ning Xiang, and Zhenhua Huang. Environmental issues associated with wind energy – a review. *Renewable Energy*, 75:911 – 921, 2015.

[51] A. Khamis, Z. M. Badarudin, A. Ahmad, A. A. Rahman, and N. A. Bakar. Development of mini scale compressed air energy storage system. In *2011 IEEE Conference on Clean Energy and Technology (CET)*, pages 151–156, June 2011.

[52] G. F. C. (Gordon Frederick Crichton) Rogers. *Engineering thermodynamics, work and heat transfer*. Longman, Harlow, 4th ed. edition, 1992.

[53] V. Vongmanee and V. Monyakul. A new concept of small-compressed air energy storage system integrated with induction generator. pages 866–871. IEEE, November 2008.

[54] Arsie II, Marano VV, Nappi GG, and Rizzo GG. A model of a hybrid power plant with wind turbines and compressed air energy storage. volume ASME 2005 Power Conference. ASME, 2005.

[55] J. P. (Jack Philip) Holman. *Heat transfer*. McGraw-Hill series in mechanical engineering. McGraw Hill Higher Education, Boston, 10th ed. edition, 2010.

[56] T.E.W. Schumann. Heat transfer: A liquid flowing through a porous prism. *Journal of the Franklin Institute*, 208(3):405 – 416, 1929.

[57] Steven Stoft. *Power system economics : designing markets for electricity*. Wiley-Academy, New York, 2001.

[58] Joseph C. Hartman. *Engineering economy and the decision-making process*. Pearson/Prentice Hall, Upper Saddle River, N.J., 2006.

[59] ASIMPTOTE. *Cycle Tempo Operation Manual*. Accessed on: 25-06-19.

[60] Inc. The Mathworks. *Simscape User's Guide 2018a*. Accessed on 27-06-19.

[61] Fei Wang, Kangping Li, Lidong Zhou, Hui Ren, Javier Contreras, Miadreza Shafie-khah, and João P.S. Catalão. Daily pattern prediction based classification modeling approach for day-ahead electricity price forecasting. *International Journal of Electrical Power & Energy Systems*, 105:529 – 540, 2019.

[62] https://airsquared.com/products/scroll-expanders/.

[63] R. E. Patton. Gas turbine operation in extreme cold climates. *ASME 1976 International Gas Turbine and Fluids Engineering Conference*, Volume 1B: General, 1976.

[64] D. Handley and P.J. Heggs. The effect of thermal conductivity of the packing material on transient heat transfer in a fixed bed. *International Journal of Heat and Mass Transfer*, 12(5):549 – 570, 1969.

[65] https://www.nordpoolgroup.com/.

[66] Henry hub natural gas spot price. https://www.eia.gov/dnav/ng/hist/rngwhhdD.htm.

[67] LG. Resu 3.3 battery pack specification. Technical report, LG, 2016.

[68] Andrew Smallbone, Verena Jülch, Robin Wardle, and Anthony Paul Roskilly. Levelised cost of storage for pumped heat energy storage in comparison with other energy storage technologies. *Energy Conversion and Management*, 152:221 – 228, 2017.

[69] B. Zhou, S. Liu, S. Lu, X. Cao, and W. Zhao. Cost–benefit analysis of pumped hydro storage using improved probabilistic production simulation method. *The Journal of Engineering*, 2017(13):2146–2151, 2017.

[70] D. Steward, G. Saur, M. Penev, and T. Ramsden. Lifecycle cost analysis of hydrogen versus other technologies for electrical energy storage. Technical report, National Renewable Energy Laboratory, November 2009.

[71] Marcus Budt, Daniel Wolf, Roland Span, and Jinyue Yan. Compressed air energy storage – an option for medium to large scale electrical-energy storage. volume 88, pages 698–702. Elsevier Ltd, June 2016.

[72] Joern Buss and Tobias Sitte. Tailored product cost down for industrial products and equipment, November 2014. Accesed on: 2nd July 2019.

[73] Y.M. Kim and D. Favrat. Energy and exergy analysis of a micro-compressed air energy storage and air cycle heating and cooling system. *Energy*, 35(1):213 – 220, 2010.

[74] Ayad M. Al Jubori and Qusay A. Jawad. Investigation on performance improvement of small scale compressed-air energy storage system based on efficient radial-inflow expander configuration. *Energy Conversion and Management*, 182:224 – 239, 2019.

[75] Xinjing Zhang, Yujie Xu, Xuezhi Zhou, Yi Zhang, Wen Li, Zhitao Zuo, Huan Guo, Ye Huang, and Haisheng Chen. A near-isothermal expander for isothermal compressed air energy storage system. *Applied Energy*, 225:955 – 964, 2018.

[76] Robert Mendick. Wind farms paid 100m to switch power off. https://www.telegraph.co.uk/news/2018/01/08/wind-farms-paid-100m-switch-power/, January 2018.